Arabian Journal for Science and Engineering
https://doi.org/10.1007/s13369-026-11156-7

RESEARCH ARTICLE-CIVIL ENGINEERING

CBR Performance of Geosynthetic-Reinforced Subgrades in Layered and Homogeneous Soil Systems

Nur Rasfina Mahyan[1,2] · Mastura Azmi[1] · Fauziah Ahmad[1] · Siti Noor Linda Taib[3]

Received: 26 September 2025 / Accepted: 3 February 2026

Abstract

This study systematically evaluates the effectiveness of geosynthetic reinforcement on subgrade soils prevalent in tropical climates, specifically those involving sandy, lateritic, and layered sand-over-laterite soils, through comprehensive laboratory. California bearing ratio (CBR) tests conducted under both soaked and unsoaked conditions. Reinforcements using woven geotextile and biaxial geogrid were installed at varying depths ($0.3H$, $0.4H$, and $0.5H$), enabling a detailed analysis of the placement effects on soil strength. Results indicate that the geotextile consistently outperformed the geogrid across all soil types, markedly enhancing the soaked bearing capacity, particularly in sandy soils (reinforcement ratio $\eta = 2.02$ at $0.3H$), due to its superior confinement and moisture resilience. In cohesive lateritic soils, deeper reinforcement placement ($0.5H$) provided maximum efficiency ($\eta = 1.52$), effectively controlling plastic deformation from moisture exposure. For layered configurations, placing reinforcement at the sand–laterite interface notably improved stiffness transitions, maximizing absolute bearing capacity (CBR = 13.84% at $0.5H$). Optimum reinforcement efficiency, however, occurred at shallower depths ($0.3H$). A critical trade-off between maximum strength and reinforcement efficiency was identified, emphasizing depth-specific optimization strategies tailored to individual soil behaviours. These findings significantly advance practical pavement design guidelines, providing clear, empirically based recommendations for geosynthetic type and optimal placement depth, thereby supporting the development of sustainable and resilient pavement infrastructures that align with the Sustainable Development Goals (SDG 9, SDG 11).

Keywords Geosynthetic reinforcement · Tropical subgrades · CBR · Reinforcement efficiency · Layered soil stabilization

1 Introduction

The mechanical characteristics and integrity of the underlying subgrades have a significant influence on the structural performance and longevity of pavement systems in tropical climates. This dependency is particularly critical due to the dramatic fluctuations in moisture content and the extensive variations in soil strength and stiffness caused by seasonal weather patterns. Tropical regions, including Southeast Asia, West Africa, and parts of Latin America, exhibit a diverse range of soil types, such as cohesionless sandy deposits, cohesive lateritic soils, and layered configurations that combine sand and laterite. Each soil type presents distinct geotechnical challenges that necessitate tailored approaches to achieve durable pavement foundations [1–5].

Sandy soils in tropical regions are characterized by high permeability and minimal cohesive strength, which significantly influence their behaviour and management. These soils allow rapid water infiltration due to their large pore spaces, which can be beneficial for drainage but problematic for water retention. When sandy soils become saturated, the interparticle friction decreases, leading to a significant reduction in load-bearing capacity [6, 7]. This can cause substantial deformation under vehicular loads, compromising pavement performance. Their susceptibility to moisture-induced degradation necessitates careful engineering interventions to sustain structural stability.

✉ Mastura Azmi
cemastura@usm.my

1 School of Civil Engineering, Universiti Sains Malaysia, 14300 Nibong Tebal, Malaysia

2 Centre for Pre-University Studies, Universiti Malaysia Sarawak, 94300 Kota Samarahan, Malaysia

3 Department of Civil Engineering, Universiti Malaysia Sarawak, 94300 Kota Samarahan, Malaysia

Published online: 02 March 2026

In contrast, lateritic soils, prevalent in tropical regions, exhibit unique mechanical properties due to their mineralogical composition and environmental conditions. These soils are characterized by high fines content, which results in relatively low permeability and cohesive properties. The presence of iron and aluminium oxides play a crucial role in cementing soil particles, contributing to their mechanical stability under dry conditions [8–10]. However, extended saturation can compromise these bonds, causing moderate reductions in strength and stiffness [11, 12]. The engineering complexity of lateritic soils arises not only from their susceptibility to moisture but also from their inherently heterogeneous structure, which introduces variability and uncertainty into pavement foundation design.

Adding further complexity, layered soil systems, such as sand-over-laterite, are standard in both natural settings and engineered environments. These systems are characterized by significant contrasts in stiffness and complex interfacial behaviours, which influence load transfer and deformation mechanisms [13, 14]. The interface between sand and laterite in layered soil systems is a critical zone that significantly influences the performance and durability of pavement structures. This interface can lead to stress concentration and differential settlement, which pose risks for pavement distress and premature structural deterioration [12, 15].

To mitigate these soil-related vulnerabilities, geosynthetics—particularly woven geotextiles (GT) and biaxial geogrids (GG)—have been increasingly adopted in pavement engineering practices worldwide. Geosynthetics enhance subgrade performance primarily through reinforcement mechanisms, offering confinement, tension membrane support, and interlocking interactions with adjacent soils [16–18]. These mechanisms contribute to increased service life, reduced maintenance, and base course reduction, making geosynthetics a valuable tool in geotechnical engineering. Geotextiles, due to their continuous planar structure, are particularly advantageous in soils prone to significant deformation under saturation [19, 20]. In contrast, geogrids predominantly rely on particle interlocking, making them suitable for stabilizing granular soils [21, 22]. Despite extensive use, critical gaps remain in understanding the comparative performance of geotextiles versus geogrids in layered tropical soil conditions, particularly under realistic moisture scenarios encountered in field conditions.

Significantly, the optimal depth placement of geosynthetic reinforcements within the subgrade profile remains uncertain. Recent literatures [23–28] highlight substantial variation in reinforcement effectiveness with depth; yet, comprehensive systematic assessments explicitly targeting tropical layered soils under varying moisture conditions are scarce. Past studies on geosynthetic materials and soil interactions have often focused on homogeneous soil scenarios under simplified laboratory conditions, neglecting the complex interactions typical of real-world applications involving stratified soil structures [29–33]. Consequently, current pavement design practices often lack rigorous experimental evidence to guide effective selection of reinforcement type and depth for distinct tropical subgrade scenarios.

Addressing these research gaps, the present study systematically evaluates the comparative reinforcement effectiveness of woven geotextiles and biaxial geogrids in sandy, lateritic, and layered sand-over-lateritic soils with subgrade configurations having thickness ratios of 30:70, 40:60, and 50:50 under both soaked and unsoaked conditions, using standard California bearing ratio (CBR) tests. Reinforcement layers were strategically positioned at varying depths ($0.3H$, $0.4H$, and $0.5H$) to examine the depth-specific effectiveness critically. The study aims to quantify absolute bearing capacity improvements, reinforcement efficiency (η), and moisture-related degradation behaviours to provide robust empirical guidelines for practical pavement design.

Furthermore, this research critically addresses the trade-offs between maximizing absolute subgrade strength and achieving optimal reinforcement efficiency. By explaining how the effectiveness of reinforcement varies across different soil types, moisture scenarios, and depth placements, the outcomes of this investigation significantly advance pavement reinforcement design practices. Importantly, these insights directly contribute to sustainable infrastructure development, aligning closely with global sustainability objectives, including the United Nations Sustainable Development Goals (SDGs), particularly SDG 9 (Industry, Innovation, and Infrastructure) and SDG 11 (Sustainable Cities and Communities).

Thus, the findings from this study serve not only to bridge existing knowledge gaps but also to support infrastructure development strategies by delivering practical, scientifically rigorous recommendations tailored explicitly for tropical pavement engineering contexts. This study lays a strong foundation for subsequent research efforts, encompassing large-scale cyclic plate load testing, numerical simulations under field loading scenarios, and the evaluation of long-term geosynthetic performance under tropical environmental conditions.

2 Materials and Methods

2.1 Soil Materials

Three distinct subgrade configurations were prepared to represent typical ground conditions in tropical infrastructure applications: poorly graded sandy soil (SP), lateritic clayey sand (SC), and a layered sand-over-laterite system. These soils were selected to evaluate the impact of gradation, plasticity, and layer interaction on the bearing performance of

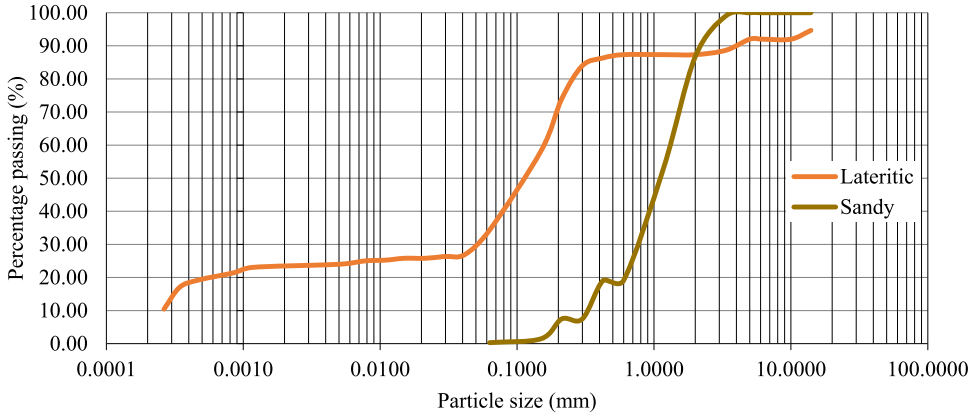

Fig. 1 Particle size distributions of lateritic and sandy soils

reinforced and unreinforced subgrades. The particle size distribution curves of the soils are shown in Fig. 1.

The sandy soil was classified as SP (poorly graded sand, A-1-b [34], with a sand fraction of 85.63%, gravel content of 14.11%, and negligible fines. Its effective grain diameter (D_{10}) was 0.51 mm, and the average particle size (D_{50}) was 1.12 mm, indicating a coarse, well-draining texture. The soil exhibited low plasticity (non-plastic), a coefficient of permeability of 0.427 cm/s, and a maximum dry density (MDD) of 1.84 Mg/m^3, compacted at an optimum moisture content (OMC) of 10.2% as shown in Fig. 2. This high permeability and cohesionless structure suggest high initial bearing strength under dry conditions but significant susceptibility to moisture-induced softening [35–37].

In contrast, the lateritic clayey sand was classified as SC (clayey sand, A-2-6, [34], containing 23.05% clay and 11.28% silt, resulting in a fine-grained matrix with a high uniformity coefficient ($C_u = 592.59$) and low permeability (2.83×10^{-7} cm/s). Its liquid limit was 33.0%, plastic limit 18.6%, and plasticity index 14.4%, confirming moderate plasticity. The soil compacted to a MDD of 1.78 Mg/m^3 at an OMC of 15.2% as shown in Fig. 2. The fine content and plasticity reflect increased cohesion [12], though these characteristics also suggest reduced permeability and potential for swelling and softening upon soaking [38, 39]. However, due to its aggregated structure and iron-alumina cementation, lateritic soil may retain structural stiffness even when partially saturated [40, 41].

The layered configuration was constructed by compacting sandy soil over lateritic clayey sand in three distinct thickness ratios: 30:70, 40:60, and 50:50 (sand: laterite by height) within the CBR mould to simulate stratified subgrades commonly encountered in tropical pavement systems. The interface behaviour between these contrasting materials was expected to influence stress transfer and deformation during penetration.

All soil samples were air-dried, pulverized, and passed through a 4.75 mm sieve before testing. Standard laboratory classification procedures were conducted in accordance with [42, 43], including grain size analysis, Atterberg limits, and the Standard Proctor compaction test. The resulting geotechnical parameters, such as particle size distributions, plasticity characteristics, dry densities, and permeability coefficients, are summarized in Table 1. These parameters were used to control sample preparation and interpret load-bearing behaviour during subsequent CBR testing.

2.2 Geosynthetic Reinforcement

Two types of geosynthetic reinforcements were used in this study: a woven polyester geotextile (GML10) and a biaxial polyester geogrid (FG100). The geosynthetic samples are shown in Fig. 3. These materials were chosen for their compatibility with the tested subgrade materials and prior evidence supporting their effectiveness in stabilizing subgrades within tropical pavement systems [44–48].

Geosynthetics are available in a wide variety of forms, materials, and geometries to suit distinct geotechnical functions, including separation, reinforcement, filtration, drainage, and protection. The selection of a geosynthetic product for subgrade reinforcement is governed by application-specific performance criteria, including material durability, mechanical strength, environmental stability, availability, and cost-effectiveness [49–53]. In subgrade applications, geogrids are primarily chosen for their reinforcement function, where their rigidity, junction strength, and aperture size promote interlock with coarse-grained particles. These properties contribute to lateral confinement and shear resistance, which are especially important for performance under repeated loading or in weak soils with low confinement capacity [54–56].

In this study, the geotextile was selected for its broad contact area and tensile membrane effect, making it particularly effective in fine-grained or layered soil systems where tensile separation and strain compatibility are critical. The geogrid was selected for its high interlock efficiency in granular

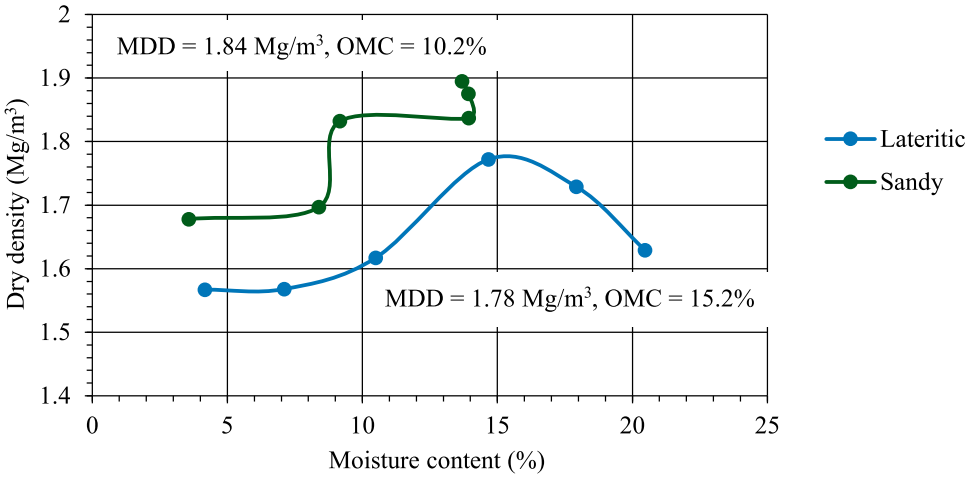

Fig. 2 Compaction curve of lateritic and sandy soils based on the standard proctor test

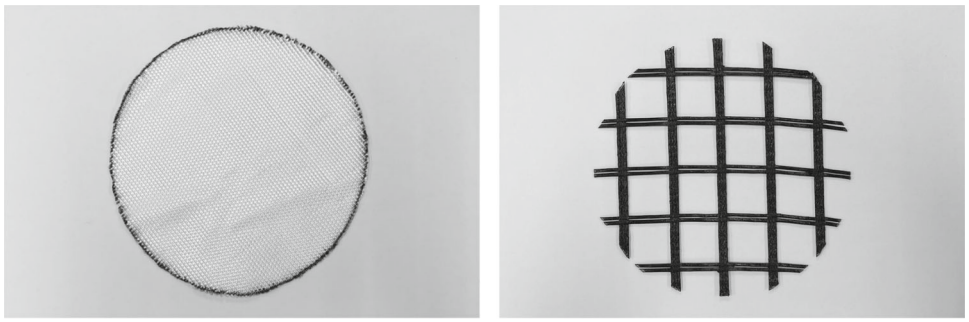

a) b)

Fig. 3 Geosynthetics used in the study: **a** GT and **b** GG

media, where its structural rigidity and open grid configuration enhance load transfer and limit deformation. Both materials were sourced from a single commercial supplier to ensure consistency in polymer composition and manufacturing quality.

The geotextile (GML10) is a woven fabric composed of UV-stabilized polyester fibres with a unit weight of 200 g/m^2. It has a tensile strength of 100 kN/m in the machine direction (MD) and 50 kN/m in the cross-machine direction (CD), with elongation values of less than 12% (MD) and 15% (CD). Its high permeability ($> 1 \times 10^{-4}$ cm/s) enables dissipation of pore pressures during loading and saturation, which is critical in maintaining interface drainage and reducing excess pore water buildup during soaked CBR testing. The material's mechanical stability and controlled deformation profile make it well-suited for both confinement and tensile membrane action in low-cohesion soils. The complete set of material parameters is provided in Table 2.

The geogrid (FG100) is a biaxial reinforcement composed of polyester yarns, designed to transfer load through aperture interlocking with adjacent soil particles. Its ultimate tensile strength reaches 100 kN/m (in the machine direction, MD) and 30 kN/m (in the cross direction, CD), with corresponding elongations of 10% in both directions. At working strains of 2% and 5%, the material provides intermediate stiffness, with tensile resistances of 20–50 kN/m in MD and 18–36 kN/m in CD. The long-term design strength (T_a) is rated at 59 kN/m, providing confidence in sustained load support applications. The geogrid features nominal aperture sizes of 21 mm (MD) and 25 mm (CD), which are suitable for interlocking with coarse-to-medium grained soils. Additional yarn properties include a carboxyl end group (CEG) concentration < 30 mmol/kg and a molecular weight exceeding 25,000 Mn, both indicating chemical resistance and long-term stability. A summary of geogrid characteristics is given in Table 3.

All geosynthetics were cut to fit the CBR mould dimensions, preconditioned in laboratory environments before testing, and placed without overlap or wrinkling at the designated reinforcement depths (0.3H, 0.4H, and 0.5H). The selection of these materials, representing two distinct reinforcement mechanisms—membrane-based (GT) and interlock-based (GG)—was made to enable a comparative assessment of their effectiveness across cohesive, non-cohesive, and layered subgrade systems.

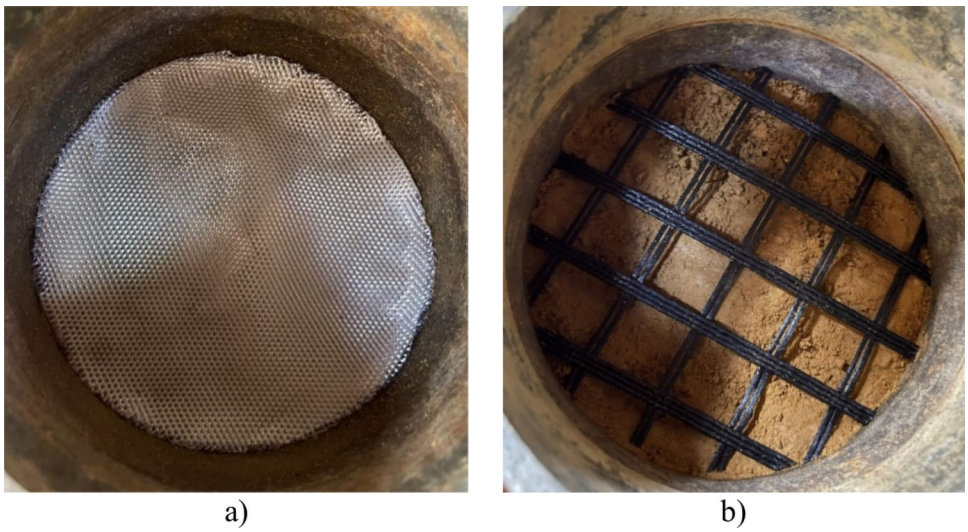

Fig. 4 Orientation of reinforcement layer positioned at a specified depth in CBR mould: **a** GT and **b** GG

Table 1 Geotechnical properties of subgrade soils

Properties	Sandy	Lateritic
Effective diameter, D_{10} (mm)	0.51	0.00027
Average diameter, D_{50} (mm)	1.12	0.12
Uniformity coefficient, C_u	2.53	592.59
Curvature coefficient, C_c	0.9	62.59
Gravel percentage (> 2 mm) (%)	14.11	7.33
Sand percentage (0.06 mm–2 mm) (%)	85.63	53
Silt percentage (0.002 mm–0.06 mm) (%)	–	11.28
Clay percentage (< 0.002 mm) (%)	–	23.05
Specific gravity, G_s	2.61	2.55
Classification (AASHTO)	A-1-b	A-2–6
Classification (USCS)	SP (poorly graded sand)	SC (clayey sand)
Liquid limit (%)	–	33.03
Plastic limit (%)	–	18.64
Plasticity Index (%)	–	14.38
Optimum moisture content (%)	10.2	15.2
Maximum dry density (Mg/m^3)	1.84	1.78
Coefficient of permeability (cm/s)	0.427	2.83×10^{-7}
Loss on ignition (%)	1.36	5.76
Unsoaked CBR (%)	13.67	3.22
Soaked CBR (%)	11.53	3.19

Table 2 Mechanical and hydraulic properties of woven geotextile (GML10)

Properties	Unit	Geotextile GML10
Weight	g/m^2	200
Tensile strength, MD	kN/m	100
Tensile strength, CD	kN/m	50
Elongation MD	%	< 12
Elongation CD	%	< 15
Permeability	cm/s	$> 1 \times 10^{-4}$
Raw material		Polyester
UV stability		UV stabilized

2.3 Sample Preparation and Testing

The CBR test was conducted for this study to evaluate the bearing strength of reinforced and unreinforced subgrade soils under both soaked and unsoaked conditions. All procedures followed the specifications of [57]. The standard CBR mould used had an internal diameter of 152 mm and a height of 127 mm. Subgrade materials were prepared by calculating the required dry weight based on the MDD, and water corresponding to the OMC was added to achieve uniform mixing. The soil was compacted in five equal layers using the Standard Proctor method. The reinforcements were cut into circular discs slightly smaller than the internal diameter of the mould, as shown in Fig. 4, to prevent edge contact or folding during compaction.

To capture the effect of geosynthetic type, placement depth, and soil profile, 14 main configurations were tested for each reinforcement material across the three subgrade conditions: sandy soil, lateritic soil, and layered sand-over-laterite. Each test was repeated for statistical consistency.

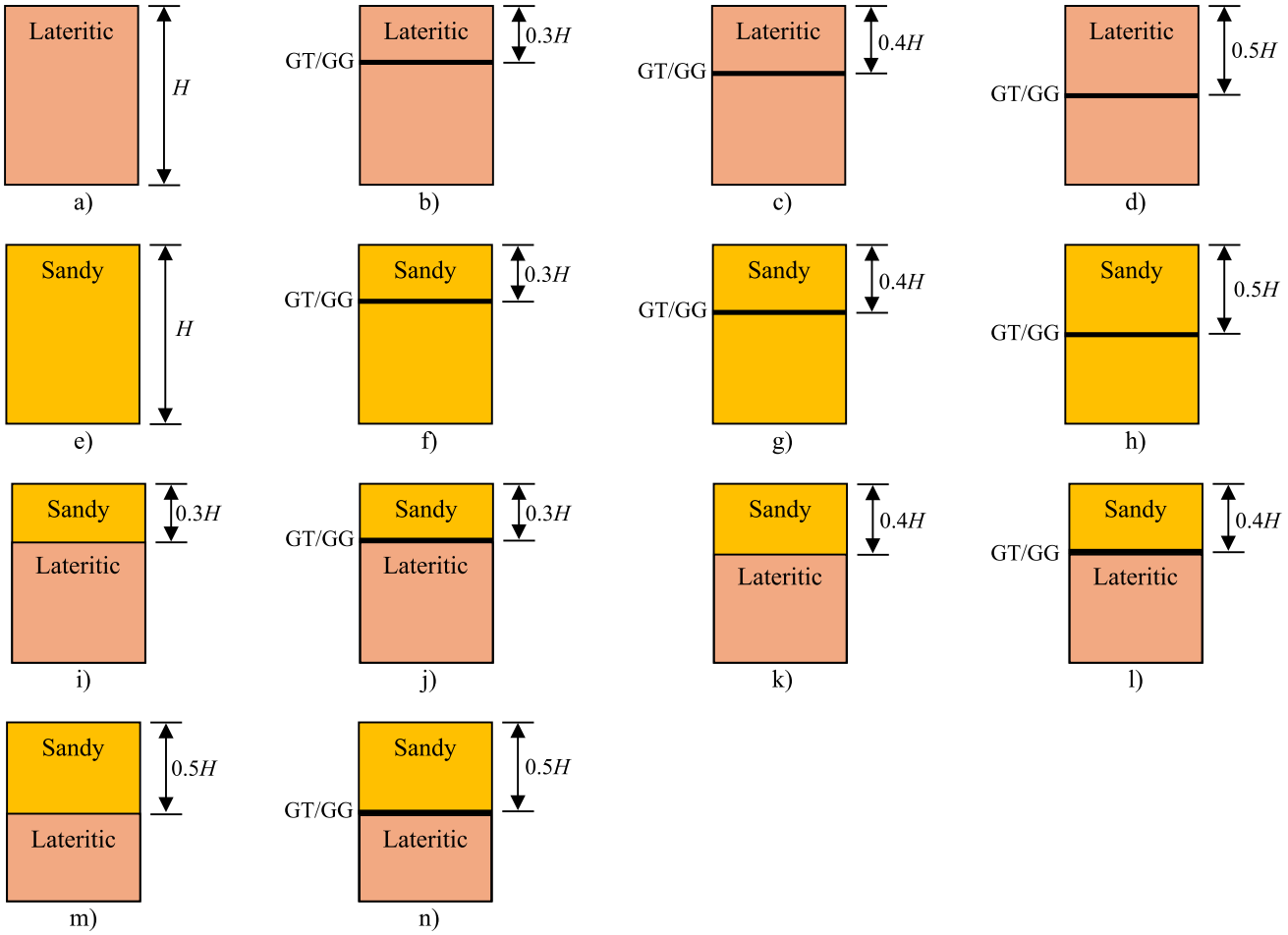

Fig. 5 Schematic illustration of GT and GG placement depths in CBR moulds: **a** unreinforced lateritic, **b** reinforced lateritic at 0.3*H*, **c** reinforced lateritic at 0.4*H*, **d** reinforced lateritic at 0.5*H*, **e** unreinforced sandy, **f** reinforced sandy at 0.3*H*, **g** reinforced sandy at 0.4*H*, **h** reinforced sandy at 0.5*H*, **i** unreinforced 30:70 sand-over-laterite, **j** reinforced 30:70 sand-over-laterite at interface, **k** unreinforced 40:60 sand-over-laterite, **l** reinforced 40:60 sand-over-laterite at interface, **m** unreinforced 50:50 sand-over-laterite, and **n** reinforced 50:50 sand-over-laterite at interface

A detailed visual overview of the test configurations is presented in Fig. 5, which illustrates the position of geotextile and geogrid layers for each depth and subgrade system. The schematic includes unreinforced profiles and each reinforced variant for both homogeneous and layered samples (sand-over-laterite in 30:70, 40:60, and 50:50 thickness ratios), enhancing experimental transparency and replicability.

In reinforced specimens, geosynthetics were placed horizontally at predetermined depths of 0.3*H*, 0.4*H*, and 0.5*H* from the top of the mould, where *H* is the mould height. These depths were selected based on experimental and theoretical evidence showing that the upper half of a CBR specimen contains the primary shear zone and the highest stress concentration during penetration. Reinforcement positioned in this region can more effectively mobilize tensile membrane action and intercept lateral deformation before it propagates downward. Previous studies on geosynthetic-reinforced CBR and subgrade systems have reported that placing reinforcement between approximately 0.25*H* and 0.50*H* results in the greatest improvement in load–penetration response and bearing capacity [58–61]. This strategy enhances soil stability, bearing capacity, and reduces settlements, making it a cost-effective and efficient solution for various geotechnical applications. The placement of geosynthetic reinforcement at the interface between the upper sandy layer and the underlying lateritic soil in a layered sand-over-laterite configuration is a strategic approach to address stiffness discontinuities and stress concentrations at material boundaries [25, 33, 62, 63]. This method is particularly relevant in field conditions where contrasts in shear strength and permeability can lead to stress concentrations. By reinforcing this transitional zone, the geosynthetic effectively facilitated stress redistribution, minimized potential slip or differential settlement across the

Table 3 Mechanical, structural, and material properties of biaxial geogrid (FG100)

Properties	Unit	Geogrid FG100
Tensile strength (ultimate), MD	kN/m	100
Tensile strength (ultimate), CD	kN/m	30
Elongation, MD	%	10
Elongation, CD	%	10
Tensile strength at 2% strain, MD	kN/m	20
Tensile strength at 2% strain, CD	kN/m	18
Tensile strength at 5% strain, MD	kN/m	50
Tensile strength at 5% strain, CD	kN/m	36
Long-term design strength, T_{al}[2]	kN/m	59
Yarn properties		
Material		Polyester
Carboxyl end group (CEG)	mmol/kg	< 30
Molecular weight	Mn	> 25,000
Physical characteristics		
Roll width	m	4.0
Roll length	m	50/100
Roll area	m^2	200/400
Aperture size, MD ± 20%	mm	21
Aperture size, CD ± 20%	mm	25

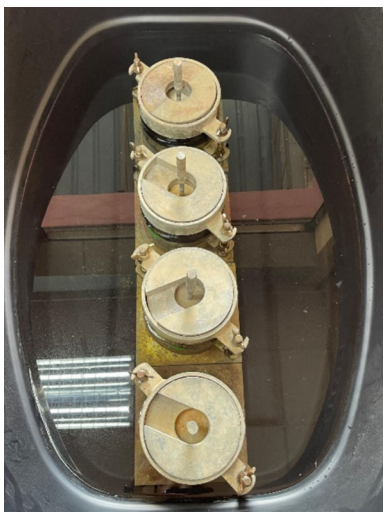

Fig. 6 Soaked samples in the immersion tank

interface, and enhanced the overall load-bearing response of the layered subgrade system.

The unsoaked samples were tested immediately after compaction, while soaked specimens were submerged in water for 96 h. Figure 6 shows the soaked samples in an immersion tank filled with water and under a surcharge. The CBR test was performed using a TRIPLEX electromechanical

Fig. 7 Experimental setup of the CBR test

loading system as shown in Fig. 7, which applied vertical force through a loading plunger at a standard penetration rate of 1 mm/min. Load–penetration data were continuously recorded using a connected load cell and linear variable displacement transducer (LVDT). The maximum force at 2.5 mm and 5.0 mm penetration was used to calculate the CBR value. Where both readings were available, the higher value was reported unless a significant deviation required comparative discussion. This setup enabled the accurate measurement of strength variation under various reinforcement and moisture conditions.

2.4 Performance Metrics

The mechanical performance of each subgrade configuration, both reinforced and unreinforced, was evaluated using two primary metrics derived from the CBR test. First, the CBR value was determined from the penetration resistance recorded at two standard depths: 2.5 mm and 5.0 mm, as specified by [57]. In accordance with international testing norms, the higher of the two values was reported, except where material heterogeneity or curve anomalies necessitated dual reporting for comparative interpretation [64–66]. To assess the benefit of geosynthetic inclusion, a reinforcement ratio (η), Eq. (1), was calculated for each configuration. This

Table 4 Unreinforced CBR performance of subgrade soils

Soil type	Unsoaked CBR (%)	Soaked CBR (%)	CBR reduction (%)
Sandy	13.67	11.53	15.65
Lateritic	3.22	3.19	0.93
Layered 30:70	5.28	4.70	10.98
Layered 40:60	6.96	6.28	9.77
Layered 50:50	11.80	10.94	7.29

dimensionless metric normalizes reinforced performance relative to an unreinforced control and is defined as:

$$\eta = \frac{\mathrm{CBR}_{\mathrm{reinforced}}}{\mathrm{CBR}_{\mathrm{unreinforced}}} \tag{1}$$

This ratio provides a direct measure of reinforcement efficiency and allows for meaningful comparisons across different soil types, moisture conditions, and placement depths. As reinforced and unreinforced tests were conducted under identical preparation and loading conditions, the η metric isolates the contribution of geosynthetics to load-bearing enhancement.

Optimality criteria were assessed using a dual-benchmark approach. For each test condition, the configuration yielding the highest absolute CBR value and the highest η value was identified. These two indicators, absolute strength and normalized improvement, were interpreted in conjunction to recommend practical reinforcement depths and material choices customized to each subgrade type. This dual-metric framework reflects current best practices in geotechnical reinforcement research and has been widely adopted in the evaluation of geosynthetic-stabilized soils under both laboratory and field conditions [67, 68].

3 Results and Discussion

3.1 Effect of Subgrade Soil Type on Unreinforced CBR Strength

The mechanical response of unreinforced subgrades varies primarily with soil type, particularly under variable moisture conditions. Figure 8 and Table 4 summarize the unsoaked and soaked CBR values for five configurations: homogeneous sandy soil, homogeneous lateritic soil, and three layered sand-over-laterite profiles (with thickness ratios of 30:70, 40:60, and 50:50). The CBR values measured at 2.5 mm and 5.0 mm penetration depths provide a quantitative assessment of baseline strength and moisture sensitivity in each case.

Among the tested soil types, sandy soil recorded the highest CBR in the unsoaked condition (13.67%), consistent with its coarse-grained, non-cohesive structure that supports dense particle packing and high frictional resistance. However, upon soaking for 96 h, its strength declined sharply to 11.53%, representing a 15.65% reduction, the highest among all specimens. This behaviour is attributed to rapid saturation, loss of suction, and collapse of particle interlock due to the high permeability and lack of fines in poorly graded sands. Similar trends have been reported by [69–72], emphasizing the moisture susceptibility of unbound granular subgrades in tropical climates.

In contrast, despite showing a lower unsoaked CBR (3.22%), lateritic soil demonstrated minimal strength loss upon soaking (3.19%), with a reduction of only 0.93%. This reflects the stabilizing influence of the soil's high fines content, reduced permeability, and the presence of cementing oxides such as iron and aluminium, which enhance aggregation and moisture resistance. This stability under soaking is supported by the findings of [12, 62, 73–75], who attribute the durability of lateritic soils to their internal aggregation, electrochemical bonding, and reduced saturation kinetics.

Layered subgrades exhibited intermediate behaviour between the two homogeneous soils. For instance, the 50:50 sand-over-laterite configuration displayed an unsoaked CBR of 11.80%, dropping moderately to 10.94% after soaking, representing a 7.29% reduction. The layered systems benefited from the surface stiffness of sand and the underlying moisture resistance of laterite. In particular, the modest CBR reduction in the 50:50 sample can be attributed to the composite effect of the layered subgrade system. This effect is characterized by the upper sand layer absorbing the initial load and partial moisture, while the underlying laterite layer delays saturation and reinforces the composite system. Similar strength retention trends were observed in the 40:60 and 30:70 configurations, with CBR reductions of 9.77% and 10.98%, respectively, indicating that transitional performance is governed by interface behaviour. These observations support the conclusions of [76–80], which have demonstrated that layered subgrades benefit from stiffness contrasts and staged saturation, jointly stabilizing the soil-reinforcement interface during wetting.

Overall, the data indicate that CBR performance in unreinforced subgrades is not solely dependent on dry-state strength but is also significantly affected by soil gradation, permeability, and the capacity to retain suction under saturation. The findings emphasize the need for subgrade-specific reinforcement strategies, particularly in tropical pavement design, where moisture ingress is common and soil response is varied.

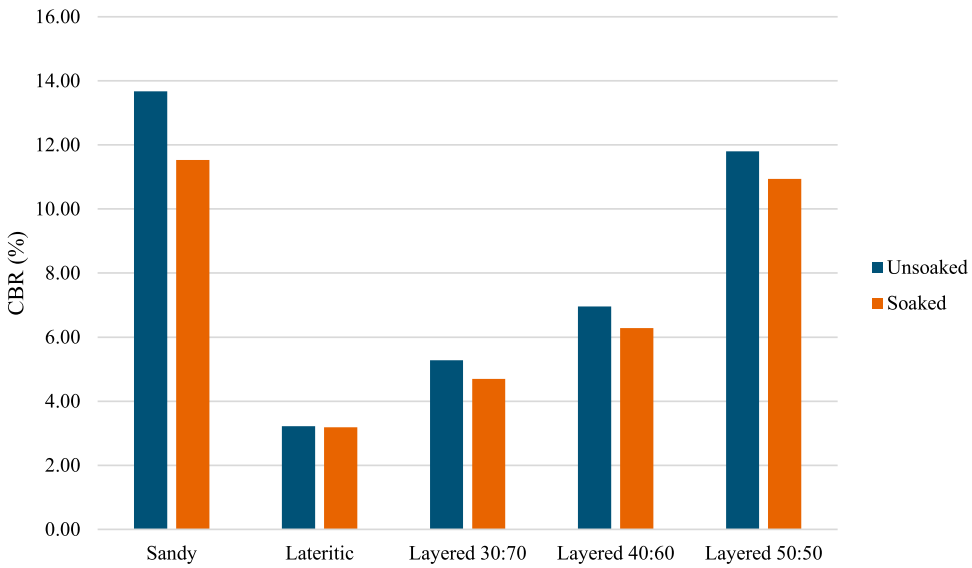

Fig. 8 Comparison of soaked and unsoaked CBR values for unreinforced sandy, lateritic, and layered sand-over-laterite subgrades

3.2 Optimization of Reinforcement Depth

The effectiveness of geosynthetic reinforcement in improving subgrade performance is strongly influenced by its placement depth, particularly in relation to the location of active shear zones and the nature of the soil strata. This section investigates the effect of varying reinforcement depths: 0.3H, 0.4H, and 0.5H, where H is the total height of the CBR mould across three subgrade systems (sandy, lateritic, and layered) using both GT and GG reinforcement.

3.2.1 CBR Performance Trends by Depth and Reinforcement Type

As illustrated in Fig. 9, GT-reinforced sandy soils achieved the highest CBR at 0.3H (23.24%), with values decreasing to 18.34% and 14.45% at 0.4H and 0.5H, respectively. This trend is consistent with the well-established understanding that in cohesionless soils, the majority of shear deformation occurs near the surface. Reinforcement placed at shallow depths effectively confines lateral expansion and intercepts shear planes early [81–83]. Similar behaviour was observed for GG-reinforced sandy soil. However, absolute CBR values were lower, at 18.80% at 0.3H, likely due to reduced interlock efficiency between the grid structure and granular particles.

In lateritic soils, which are cohesive and moisture-sensitive, both GT and GG exhibited an increasing CBR with increasing reinforcement depth. Peak strength occurred at 0.5H (4.84% for GT and 4.30% for GG), reflecting the location of the failure plane and the importance of tensile membrane effects at greater depths. Deeper placement also delays the mobilization of plastic deformation under penetration loading, especially critical in soaked lateritic profiles [46, 60, 84, 85]. The superiority of geotextile in this context is likely due to its higher contact area and better interface bonding with cohesive soils.

For layered sand-over-laterite subgrades (50:50 thickness ratio), both GT and GG produced the highest CBR values when reinforcement was placed at 0.5H (13.84% for GT and 11.92% for GG). In this configuration, 0.5H corresponds to the sand–laterite interface, making it the most strategic location to bridge the stiffness transition between layers. Reinforcement at this interface effectively controls interfacial shear, mitigates slippage, and facilitates composite action by anchoring load transfer from the upper sand to the lower lateritic layer. Similar interfacial mechanics were reported by [46, 86–89], where subgrade performance was enhanced when reinforcement aligned with vertical stiffness contrasts.

3.2.2 Reinforcement Efficiency Based on η Trends

Figure 10 presents the reinforcement ratio across reinforcement depths for all subgrade types under soaked conditions. In sandy soils, η peaked at 0.3H for both materials, with GT achieving 2.02 and GG 1.63, affirming the advantage of shallow placement in cohesionless soils where vertical stresses are concentrated near the surface. As the placement depth increased, η values declined, demonstrating reduced confinement and tensile mobilization farther from the active shear zone [90–92].

In contrast, lateritic soils exhibited increasing η values with depth. GT recorded a maximum η of 1.52 and GG 1.35 at 0.5H, corresponding to improved interaction with the deeper-seated failure plane common in cohesive, moisture-sensitive soils. This is consistent with the literature, which suggests that reinforcement in such materials should be placed closer to the critical shear zone to maximize tensile engagement and reduce moisture-related plastic deformation [12, 93–96].

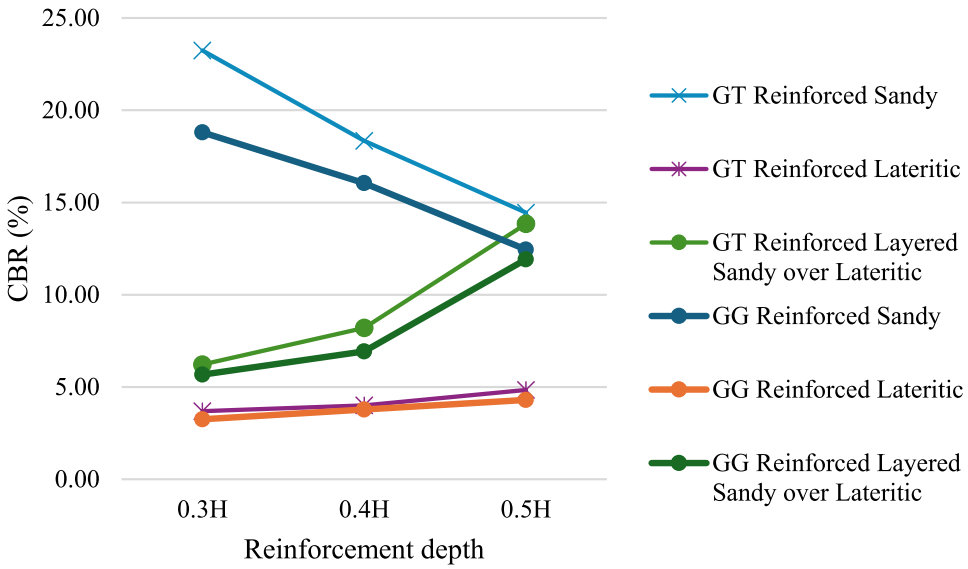

Fig. 9 Variation of CBR values with reinforcement depth for sandy, lateritic, and layered sandy over lateritic subgrades reinforced with GT and GG

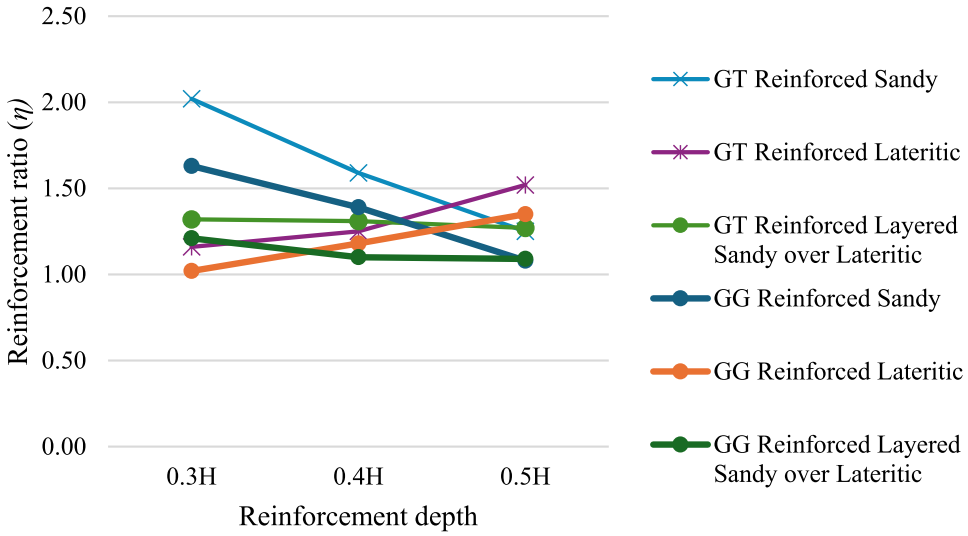

Fig. 10 Reinforcement ratio versus reinforcement depth across soil types reinforced with GT and GG

For layered sand-over-laterite subgrades, η was highest at $0.3H$ with GT (1.32) and GG (1.21). This suggests that the primary shear zone in the layered configuration remains concentrated near the sand–laterite interface under soaked conditions. In this study, both geotextile and geogrid were consistently placed at this interface across all layered configurations (30:70, 40:60, and 50:50), enabling direct interaction with the transitional stress region. The highest reinforcement efficiency observed at $0.3H$ confirms that this placement successfully mobilized the membrane effect in GT and the interlocking mechanism in GG. As the sand thickness increased, η values declined, likely due to reduced shear stress transmission reaching the reinforcement plane. These findings underscore the effectiveness of interface-level reinforcement. Still, its efficiency depends not only on placement but also on the relative contribution of the overlying material to the stress path and failure envelope [84, 97, 98].

Thus, the design implications are summarized as follows:

- Sandy soils benefit most from shallow reinforcement ($0.3H$) due to near-surface shear concentration.
- Lateritic soils require deep reinforcement ($0.5H$) to control moisture-softening and plastic deformation.
- Layered systems show best CBR strength when reinforced at the sand–laterite interface ($0.5H$), although η optimization may favour slightly shallower placement ($0.3H$) depending on the loading regime.

These results validate that reinforcement depth should not be uniformly assigned across soil systems. Instead, design decisions must reflect soil type, expected failure mechanism, and geometric stratigraphy to maximize reinforcement efficiency and long-term performance.

Table 5 CBR performance and reinforcement efficiency of GG and GT reinforcements for each soil type at their optimal depths

Soil type	Unreinforced CBR (%)	GT-reinforced CBR (%)	GG-reinforced CBR (%)	η (GT)	η (GG)	Optimum depth
Sandy	11.53	23.24	18.80	2.02	1.63	0.3H
Lateritic	3.19	4.84	4.30	1.52	1.35	0.5H
Layered 50:50	10.94	13.84	11.92	1.27	1.09	0.5H

3.3 Influence of Reinforcement Type on CBR Enhancement

The type of geosynthetic reinforcement significantly affects the magnitude of strength enhancement achieved in subgrade soils, particularly under soaked conditions where the subgrade's structural integrity is most vulnerable. This section presents a comparative evaluation of GT and GG performance across sandy, lateritic, and layered sand-over-laterite (50:50) subgrades. Performance was evaluated based on CBR values and η as tabulated in Table 5. All tests were performed at the previously optimized reinforcement depths, 0.3H for sandy soils and 0.5H for both lateritic and layered systems.

3.3.1 CBR Performance at Optimum Depth

As illustrated in Fig. 11, GT consistently achieved higher CBR values than GG across all tested configurations. In sandy subgrade, GT-reinforced samples exhibited the highest soaked CBR of 23.24%, followed by GG at 18.80%, compared to 11.53% for the unreinforced case. This substantial improvement confirms that GT's full-plane tensile stiffness and surface confinement enable it to counteract lateral strain more effectively than the discrete interlocking mechanism of GG. These findings align with [99–102], who reported that planar reinforcements outperform grid structures in cohesionless soils due to better stress dispersion and minimal void redistribution under soaked conditions.

In lateritic subgrades, GT and GG achieved CBR values of 4.84% and 4.30%, respectively, relative to an unreinforced baseline of 3.19%. Although the absolute strength gain was modest due to the cohesive and plastic nature of the soil, GT again proved superior. The geotextile's finer pore structure and continuous contact interface enhanced resistance to moisture-induced shear softening, a critical factor for tropical clays and residual soils [46, 84, 85, 103, 104]. GG, while effective in granular matrices, exhibited lower stiffness interaction under soaked cohesive conditions.

In the layered sand-over-laterite (50:50) configuration, GT achieved a soaked CBR of 13.84%, while GG followed closely at 11.92%, compared to 10.94% for the unreinforced control. Both reinforcements were placed at the sand–laterite interface (0.5H). The superior performance of GT in this case reflects its ability to bridge stiffness contrasts, ensuring better vertical load continuity and mitigating settlement discontinuities at the material interface [105–108]. GG's relatively open structure limits interfacial engagement, particularly in stratified systems where aggregate contact is irregular.

3.3.2 Reinforcement Ratio (η) Trends

The comparative reinforcement ratios presented in Fig. 12 further support these findings. Geotextile achieved η values of 2.02, 1.52, and 1.27 for sandy, lateritic, and layered soils, respectively, each exceeding the geogrid equivalents of 1.63, 1.35, and 1.09. These values indicate that GT is consistently more effective than GG, both in absolute CBR improvement and relative reinforcement efficiency. GT's continuous membrane behaviour offers superior confinement, especially under saturated loading. This was particularly evident in sandy soils, where its tensile reinforcement resists lateral dilation, and in lateritic soils, where its frictional interaction stabilizes the soil matrix against post-yield softening. GG's η dropped more significantly in cohesive and layered systems, reflecting its dependency on mechanical interlock, which becomes compromised in moisture-sensitive or finer-grained matrices. The efficiency reduction from sandy to layered and lateritic soils highlights that GG performance is highly soil-dependent, and its use in layered or cohesive tropical soils should be evaluated with caution [21, 109–111].

The comparative results confirm that GT reinforcement is generally preferred for tropical subgrade systems with varied soil stratigraphy and moisture exposure. Its performance is driven by:

- Superior membrane action under shear load,
- Consistent contact stress distribution,
- Moisture resilience and tensile stiffness across both granular and cohesive layers.

For high-stress, moisture-variable applications, GT offers more reliable and efficient reinforcement. GG may still be effective in well-graded, dry, granular fills where interlock can be fully mobilized; however, it is less effective in lateritic or layered systems under soaked conditions.

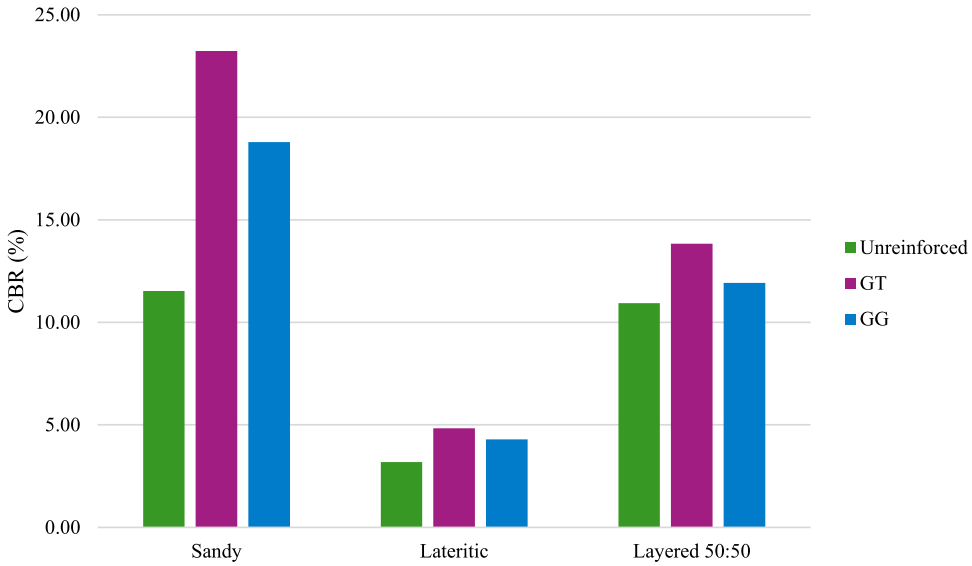

Fig. 11 CBR performance comparison for unreinforced, geotextile-reinforced (GT), and geogrid-reinforced (GG) subgrades at optimum reinforcement depth for each soil type

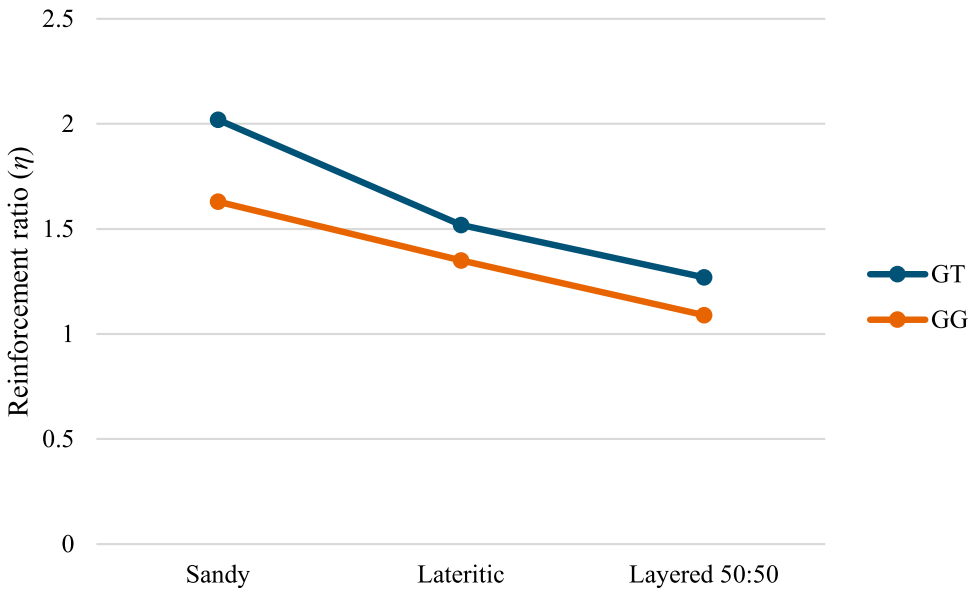

Fig. 12 Reinforcement ratio comparison between GT and GG across subgrade types at optimal depth

3.3.3 Trade-Offs Between CBR and η

This study reveals a vital design insight where maximum η does not always correspond with the highest CBR value. For example, in the layered system, the CBR peaked at 13.84% (GT at 0.5H), but η peaked at 1.32 (GT at 0.3H). This indicates that while deeper placement may yield stronger overall resistance, it does so at the cost of efficiency relative to the unreinforced case. Conversely, a high η at shallower depths may reflect better stress engagement but less total strength gains due to limited mobilization. From a design standpoint, this trade-off must be balanced based on performance objectives:

- For light-traffic pavements, maximizing η may suffice.
- For heavily loaded or wet environments, absolute CBR becomes more critical, favouring deeper placements.

3.3.4 Design Implications for Tropical Subgrades

These findings have direct implications for tropical road infrastructure:

- Sandy soils: Reinforcement should be placed at 0.3H to maximize both strength and efficiency.
- Lateritic soils: Placement at 0.5H is ideal to counteract saturation-related strength reduction.
- Layered systems: Reinforcement at the sand–laterite interface remains optimal; however, designers should consider

whether the goal is maximum strength or maximum material efficiency, as these may occur at different depths.

Furthermore, the consistent superiority of GT over GG across all configurations highlights the recommendation that geotextiles should be prioritized in soaked and composite soil environments, particularly where moisture resilience and full-plane tensile action are necessary [112–114].

3.4 Effect of Soaking on Reinforcement Efficiency

Subgrade performance under saturated conditions is a critical consideration for pavement structures in tropical regions, where heavy rainfall and seasonal wetting cycles are common. This section evaluates the impact of soaking on the strength and durability of geosynthetic-reinforced subgrades by analysing the CBR retention index (%), which is calculated as the ratio of the soaked CBR value to the unsoaked CBR value. The comparison is based on three soil types, sandy, lateritic, and layered (sand-over-laterite 50:50), reinforced with GT and GG at previously determined optimal depths.

3.4.1 Moisture Sensitivity and Retention Trends

As summarized in Table 6 and illustrated in Fig. 13, geotextile consistently achieved higher CBR retention across all soil types. In lateritic soil, GT retained 98.78% of its unsoaked strength, compared to 92.67% for GG. This suggests that even in fine-grained, low-permeability soils, GT enhances shear resistance and stiffness preservation, likely due to superior tensile support and better interface bonding [115–119]. Lateritic soils are naturally moisture-resistant due to their compacted microstructure and oxide cementation; however, the choice of reinforcement still influences post-soaking performance.

In sandy soils, where rapid saturation leads to structural breakdown of the grain matrix, GT retained 95.25%, while GG dropped to 89.40%. This notable difference (+ 5.85%) demonstrates GT's superior ability to maintain load-bearing capacity in permeable, cohesionless media. The continuous membrane action of GT inhibits lateral displacement and stress redistribution more effectively than the discrete apertures of GG, which are prone to interface softening when saturated [82, 120–124].

For the layered system, GT and GG retained 97.46% and 94.01%, respectively. The moderate retention gap (+ 3.45%) highlights GT's benefit in bridging the sand–laterite interface, which is a zone of vertical stiffness discontinuity. By controlling differential settlement and modulating vertical stress transfer across the interface, GT delays moisture-induced shear propagation from the upper sand layer to the more stable lateritic base [125–130].

3.4.2 Performance Implications

These results emphasize that the type of reinforcement matters across all soil profiles under soaked conditions, not only in moisture-vulnerable sandy soils but also in naturally resilient lateritic and composite subgrades. While both GT and GG improve CBR retention, the magnitude of preservation achieved with GT is consistently higher, confirming its enhanced mechanical interaction under saturated loading.

GT's advantages stem from:

- Higher tensile stiffness and ductility under wet deformation,
- Better full-plane soil contact for confinement,
- Resistance to interfacial weakening and migration of fines.

GG remains a viable option, particularly in dry or granular conditions, but its performance is more susceptible to degradation under soaking due to reduced confinement capacity and discontinuous stress engagement.

3.5 Load–Penetration Behaviour

Load–penetration behaviour captures the progressive stress–strain response of subgrades subjected to static penetration, providing critical insights into stiffness evolution, yielding, and energy dissipation across both reinforced and unreinforced systems. Unlike single-point CBR values, force–penetration profiles enable direct visualization of pre-yield stiffness, peak load resistance, and post-yield ductility. These elements are crucial for evaluating the full mechanical benefit of geosynthetic inclusion, particularly under variable moisture regimes and multi-layered configurations. Figures 14, 15, 16, 17, 18 and 19 illustrate this behaviour for sandy, lateritic, and layered sand-over-laterite subgrades, reinforced with GT or GG at three depths ($0.3H$, $0.4H$, and $0.5H$) under both unsoaked and soaked conditions.

3.5.1 Sandy Subgrades

Sandy subgrades demonstrated a pronounced initial stiffness, consistent with friction-dominated load transfer and minimal cohesive bonding as shown in Fig. 14. GT reinforcement at $0.3H$ yielded the highest peak force (6730 N), with a distinct curve separation compared to the unreinforced profile (3771 N). GG at $0.3H$ followed closely (5802 N), though with earlier softening beyond 5 mm penetration. As reinforcement was embedded deeper ($0.5H$), the benefit diminished, affirming the critical role of placing reinforcement in zones of high shear demand, which is typically within the top 1/3 of the specimen height [24, 84, 131].

Table 6 Comparison of unsoaked and soaked CBR values and corresponding CBR retention (%) for subgrades reinforced with GT and GG

Soil type	Reinforcement	Unsoaked CBR (%)	Soaked CBR (%)	CBR retention (%)
Sandy	GT	24.40	23.24	95.25
	GG	21.03	18.80	89.40
Laterite	GT	4.90	4.84	98.78
	GG	4.64	4.30	92.67
Layered 50:50	GT	14.20	13.84	97.46
	GG	12.68	11.92	94.01

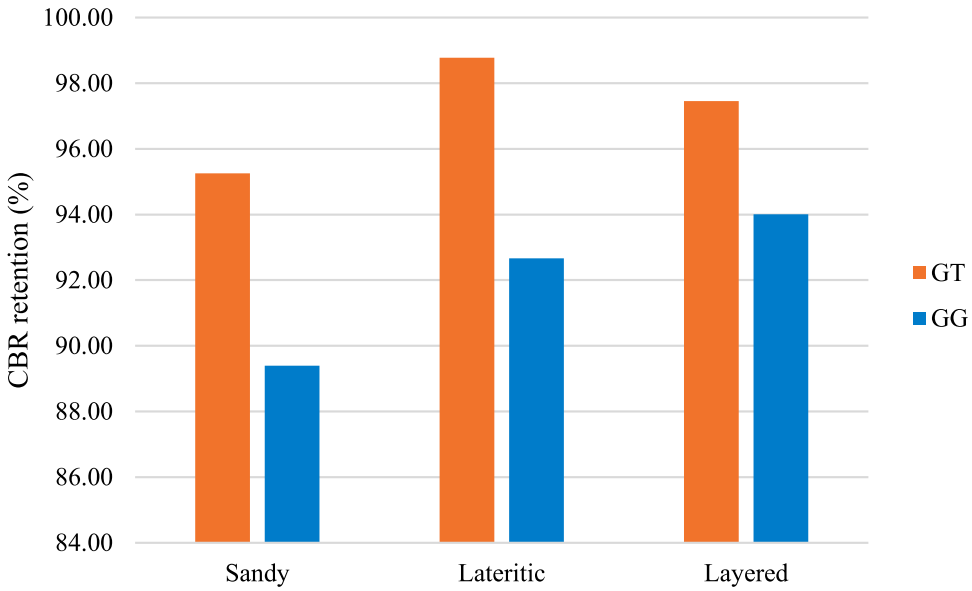

Fig. 13 CBR retention (%) under soaked conditions for GT and GG reinforcements across sandy, lateritic, and layered subgrades

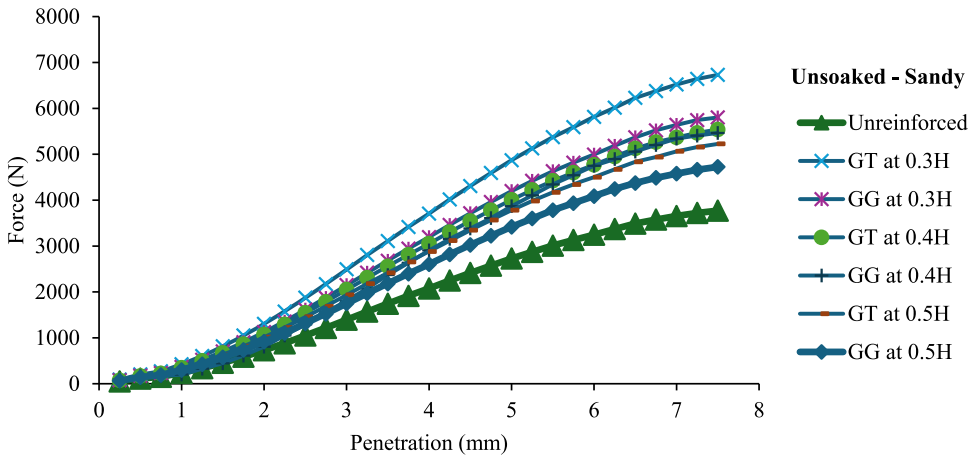

Fig. 14 Load–penetration curves for unsoaked sandy subgrade performance

The soaked specimens revealed a significant reduction in peak load capacity and curve slope, as shown in Fig. 15, highlighting the sensitivity of sandy soils to saturation-induced frictional collapse. The unreinforced sample declined to 3180 N. However, GT at 0.3*H* retained a robust load profile (6526 N), indicating effective confinement despite the development of pore pressure. GG performance also declined but retained functional stiffness (5185 N). The performance hierarchy (GT > GG > Unreinforced) persisted, with the GT curve exhibiting delayed yield, attributed to its tensile membrane action and uninterrupted soil contact [132–134].

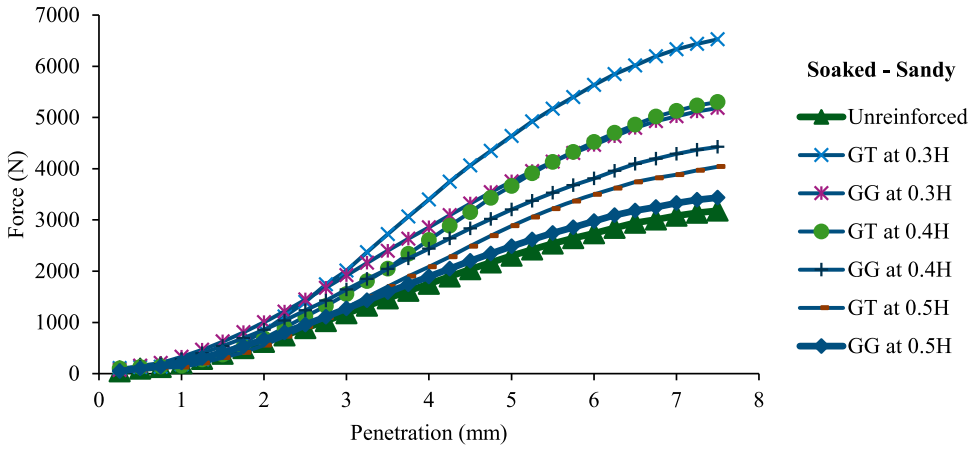

Fig. 15 Load–penetration curves for soaked sandy subgrade performance

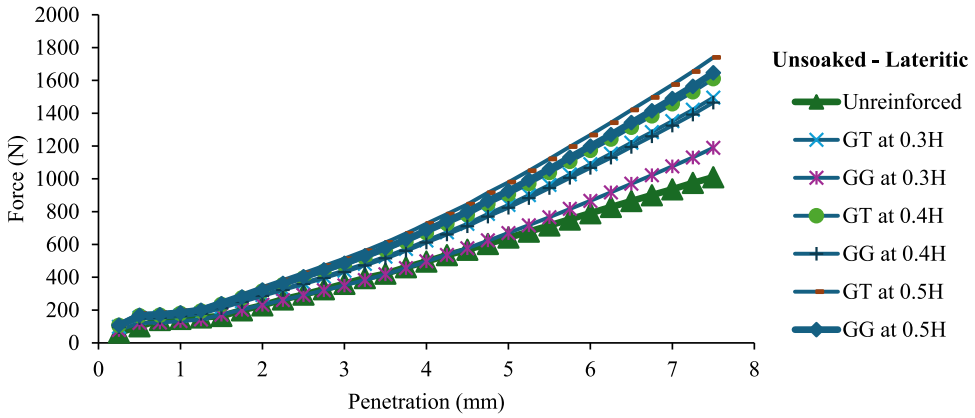

Fig. 16 Load–penetration curves for unsoaked lateritic subgrade performance

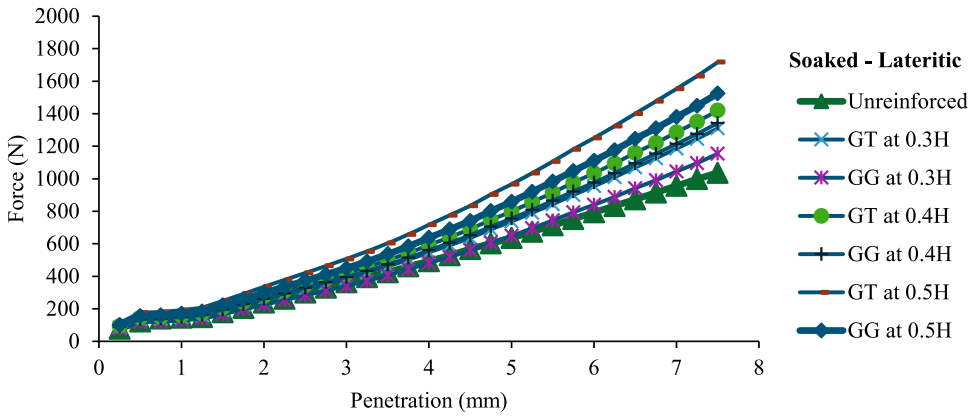

Fig. 17 Load–penetration curves for soaked lateritic subgrade performance

3.5.2 Lateritic Subgrades

Lateritic soils exhibited a gradual curve profile, as shown in Fig. 16, characterized by lower stiffness but enhanced ductility. GT reinforcement at 0.5*H* outperformed all other cases (1740 N), while GG reached its peak at 1646 N. The response reflects the cohesive and compacted microstructure of lateritic soils, where failure planes extend deeper and benefit from reinforcement embedded at a greater depth below the surface. Unlike sandy soils, reinforcement at 0.3*H* was less effective, highlighting the influence of reinforcement–failure plane alignment in fine-grained soils [12, 135, 136].

The drop in peak load, as shown in Fig. 17, was relatively modest due to the inherent low permeability and suction-retaining structure of lateritic soils. GT at 0.5*H* still reached 1717 N, preserving nearly full capacity. GG at the same depth dropped to 1525 N. These results emphasize the advantage of GT's continuous plane in resisting local shear strain and interface degradation under wet conditions. GG, while effective in increasing bearing capacity and minimizing settlement in

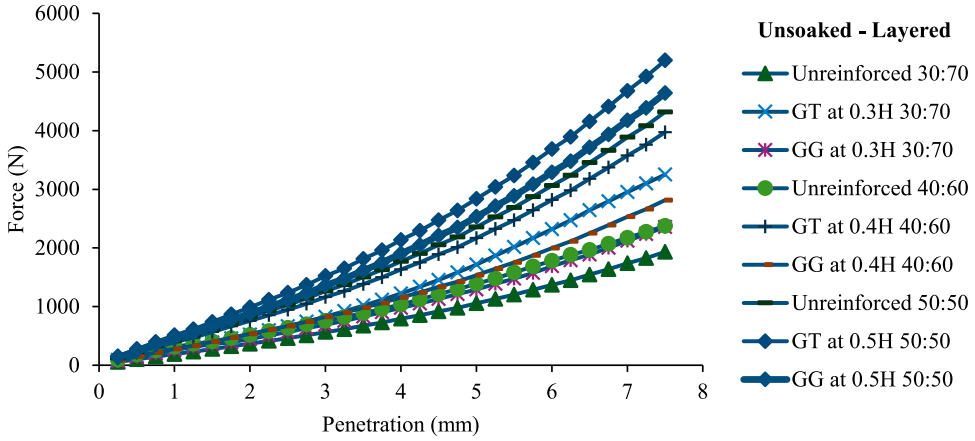

Fig. 18 Load–penetration curves for unsoaked layered subgrade performance

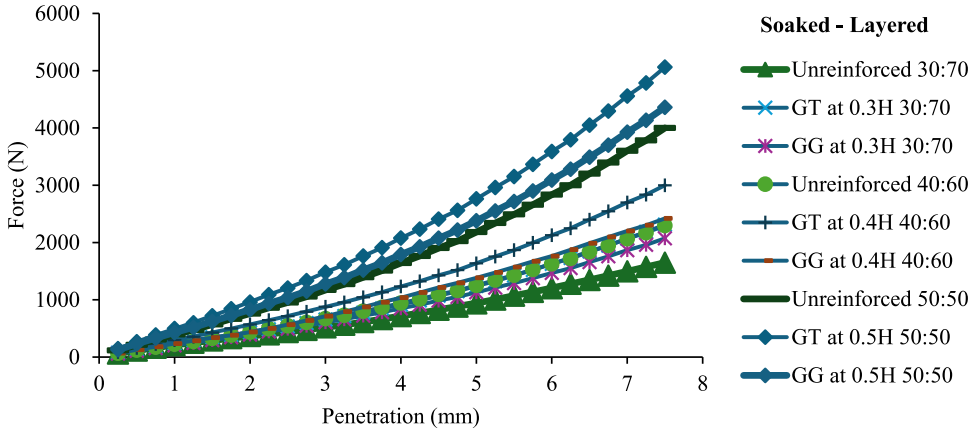

Fig. 19 Load–penetration curves for soaked layered subgrade performance

dry conditions, exhibits earlier stiffness reduction and greater deformation when saturated due to its reliance on interlock mechanisms [133, 137, 138].

3.5.3 Layered Sand-Over-Laterite Subgrades

The layered systems exhibited a bilinear load–penetration response, as shown in Fig. 18, driven by the stiffness contrast between the sandy upper layer and the lateritic lower layer. In the 50:50 configuration, GT at 0.5*H* reached the highest peak (5196 N), with a distinct curvature shift near 4 mm, indicating the activation of the underlying laterite. GG also improved (4639 N) but was less efficient in distributing load across the material interface. Shallower placements in 30:70 and 40:60 configurations exhibited reduced efficiency, especially for GG, due to poor stress bridging at the sand–laterite transition zone [126, 139, 140].

Saturation led to a general decrease in load capacity across all configurations, as shown in Fig. 19, but the 50:50 sample reinforced with GT at 0.5*H* maintained the highest strength (5062 N). The partial resistance of the layered soil to soaking is attributed to the delayed saturation of the lower layer and GT's enhanced bridging effect, which reduces interfacial settlement. GG reinforcement again showed earlier curvature flattening, indicative of weaker confinement and possible slippage at the soil–grid interface [21, 141, 142].

3.5.4 Reinforcement Depth and Failure Mechanics

Across all subgrades, the reinforcement depth played a critical role, especially under soaked conditions. For sandy soils, optimal performance was consistently achieved at 0.3*H*, where reinforcement intercepts early shear bands and limits its lateral spread. In contrast, lateritic soils benefited most from deeper placements (0.5*H*) due to their deeper failure planes and cohesive mobilization zones. In layered systems, GT at 0.5*H* in the 50:50 configuration consistently delivered the best outcome, validating the strategy of aligning reinforcement with the interface stress transition layer.

3.5.5 Comparative Reinforcement Behaviour

Table 7 presents the comparative summary of load–penetration response characteristics between GT and GG reinforcements across different soil types. The table highlights differences in peak load capacity, stiffness retention under soaking, depth sensitivity, and reinforcement-soil interface

Table 7 Comparative summary of load–penetration response characteristics between GT and GG reinforcements across different soil types

Aspect	GT	GG
Peak load	Higher across all soils and conditions	Moderate; improves early stiffness only
Stiffness retention	Strong under both dry and saturated states	Drops significantly under soaked conditions
Optimal depth	0.3H (sandy), 0.5H (lateritic, layered)	0.3H (sandy), less sensitive to depth in cohesive soil
Interface behaviour	Full-plane contact improves stress redistribution	Prone to interlock loss and interface slip

behaviour, emphasizing GT's superior performance under both dry and saturated conditions. These behaviours support the broader conclusion that GT is versatile and resilient, particularly under wetting conditions and in layered soil environments where vertical stress transitions are complex. GG offers value in dry, coarse-grained systems, but its effectiveness declines in finer or saturated media due to limited contact engagement and interfacial instability.

3.6 Composite Reinforcement Response in Layered Systems

Layered subgrades, particularly sand-over-laterite configurations, present a mechanically complex system where variations in stiffness, permeability, and failure envelope induce unique stress distributions. These systems are commonly used in tropical pavement infrastructure, where sandy fill is placed over residual clayey soils to enhance constructability and drainage. However, the transition zone at the sand–laterite interface remains a potential point of weakness, especially under saturated or cyclic conditions, where differential settlement and interfacial slip may compromise long-term performance.

Figures 20 and 21 illustrate the effect of varying sand-to-laterite thickness ratios, namely 30:70, 40:60, and 50:50, on both CBR values (%) and the corresponding η for GT and GG systems under soaked conditions. The results are crucial for understanding how composite reinforcement behaves under layered stress states and which configurations provide optimal load transfer efficiency.

3.6.1 CBR Performance with Varying Layer Ratios

As shown in Fig. 20, CBR values increased with increasing sand thickness for both GT and GG. GT-reinforced configurations consistently yielded higher values, with CBR rising from 6.22% at 30:70 to 13.84% at 50:50. This improvement can be attributed to:

- Enhanced confinement from a thicker granular cover,
- More favourable frictional interaction at the sand–geotextile interface,
- GT's ability to bridge stress concentrations and reduce interfacial settlement.

GG also showed improved CBR values with increasing sand content (from 5.67 to 11.92%), although the gains were less pronounced. This reflects GG's reliance on soil interlock, which becomes less effective when the reinforcement is buried beneath a thicker granular layer that absorbs the bulk of applied stress [46, 60, 143, 144].

3.6.2 Reinforcement Efficiency Across Thickness Ratios

Figure 21 reveals that the reinforcement ratio, a measure of reinforcement efficiency relative to unreinforced conditions, peaked at the 30:70 configuration, with $\eta = 1.32$ for GT and 1.21 for GG. These values indicate that both reinforcements are most effective when the sand layer is relatively thin, allowing greater stress transmission to the reinforcement plane. As the thickness ratio shifts to 40:60 and 50:50, η progressively declines for both materials. For GT, η drops to 1.27 at 50:50; for GG, to 1.09. This decline occurs despite an increase in absolute CBR strength, suggesting that the effectiveness of reinforcement becomes diluted as the overlying sand absorbs more load before it reaches the reinforcement zone.

Importantly, in this study, geosynthetic reinforcement was consistently placed at the sand–laterite interface for all thickness configurations. Therefore, the reduction in η with increasing sand cover is not due to placement error, but rather to a redistribution of the shear zone away from the interface, which reduces the mobilized tensile strain at the reinforcement plane. This outcome confirms that optimal reinforcement efficiency is achieved when the reinforcement lies within the active failure zone, and that interface-level engagement becomes less dominant as the upper layer thickens. Shear strain localizes higher in the profile [145–147].

3.6.3 Stress Bridging, Failure Localization, and Interface Control

Mechanically, GT's superior performance is attributed to its full-plane tensile resistance, which enables stress bridging across material boundaries and prevents differential settlement at the interface. These functions are most effective in configurations with thinner sand layers, where the interface lies within the primary shear zone. In contrast, GG's rib-and-node structure requires significant soil interlock and suffers

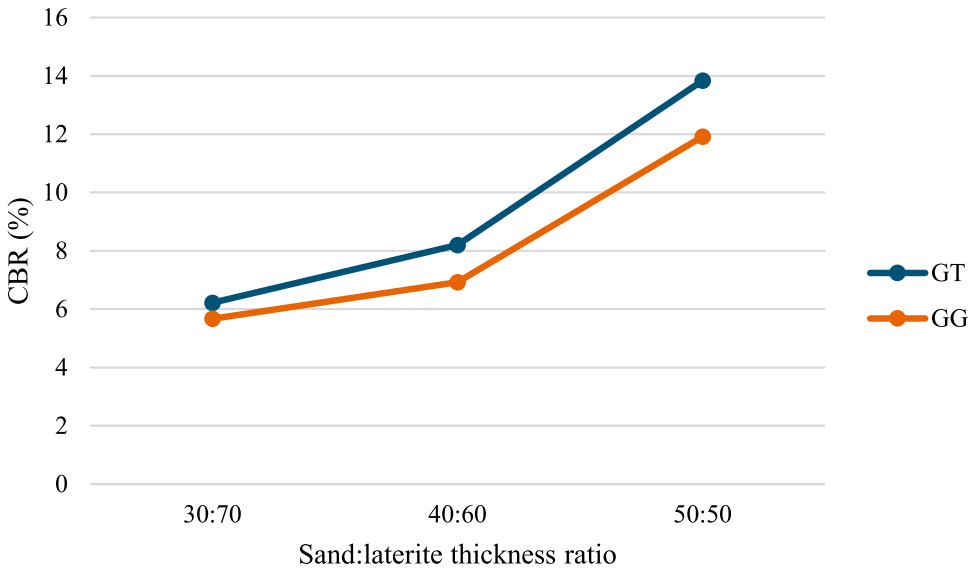

Fig. 20 Variation of CBR with sand–laterite thickness ratio for GT- and GG-reinforced systems

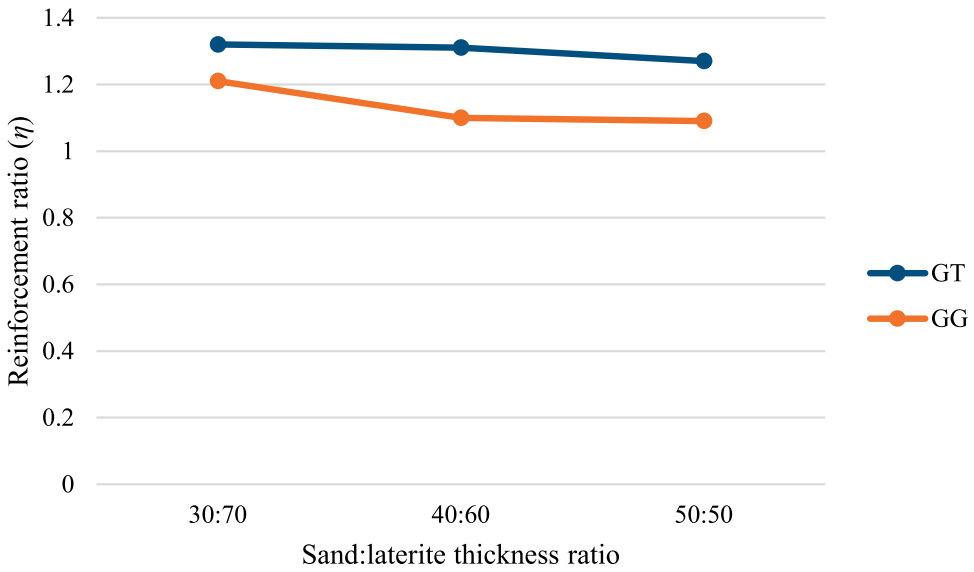

Fig. 21 Variation of η with sand–laterite thickness ratio

reduced engagement under layered and saturated conditions, especially when placed beneath thick sand strata. The findings emphasize the importance of geosynthetic placement at the correct vertical position and show that the reinforcement's influence on η is strongly linked to the location of the shear plane, which itself is governed by the geometry of the layered system.

3.7 Summary of Critical Observations

This section consolidates the most relevant findings from the comprehensive evaluation of geosynthetic-reinforced subgrades across three distinct configurations: sandy, lateritic, and layered sand-over-laterite. Key performance indicators, including optimum reinforcement depth, best-performing material, maximum CBR values, reinforcement efficiency, CBR reduction, and CBR retention, are synthesized in Table 8.

3.7.1 Consolidated Performance Summary

As shown in Table 8, GT consistently emerged as the most effective reinforcement material across all soil types, regardless of depth or saturation conditions. In sandy subgrades, the highest CBR value (23.24%) and η (2.02) were obtained at $0.3H$, confirming that tensile confinement is most effective in cohesionless soils when located near the surface [85, 148, 149]. In lateritic soils, deeper placement at $0.5H$ allowed GT to engage deeper shear planes, resulting in a peak CBR of 4.84% and η of 1.52, with a remarkable CBR retention of 98.78% despite the soil's plasticity and moisture sensitivity [60, 84, 150].

Table 8 Summary of critical observations

Soil type	Optimum depth	Best material	Max CBR (%)	η at optimum depth (GT)	CBR reduction (%)	CBR retention (%) (GT)
Sandy	0.3H	GT	23.24	2.02	4.75	95.25
Lateritic	0.5H	GT	4.84	1.52	1.22	98.78
Layered 50:50	0.5H	GT	13.84	1.27	2.54	97.46

The layered 50:50 configuration, reinforced at the sand–laterite interface (0.5H), demonstrated a balance between performance and efficiency. GT achieved a CBR of 13.84%, η of 1.27, and retained 97.46% of its unsoaked strength. These results highlight the role of interface stabilization in composite soil systems, where the reinforcement must bridge differential stiffness and modulate stress transfer [151–153].

3.7.2 Visualizing Trends: η and CBR Behaviours

Two critical performance trends are highlighted as follows:

- Fig. 8 presents a comparative analysis of soaked CBR values for unreinforced and reinforced specimens. Among the three soil systems, the sandy subgrade demonstrated the most pronounced enhancement. When reinforced with geotextile at 0.3H, the soaked CBR increased from 11.53% to 23.24%, resulting in a coefficient of variation (η) of 2.02. This indicates that the reinforcement more than doubled the bearing resistance, despite the high permeability and lack of cohesion inherent in sandy soils. This dramatic increase highlights the role of geotextiles in providing tensile confinement, resisting lateral particle movement, and preserving strength under saturated conditions [154–158]. In contrast, lateritic soil, known for its lower permeability and higher fines content, showed a modest CBR improvement from 3.19% to 4.84% under the same conditions, yielding a η of 1.52. The layered sand-over-laterite (50:50) configuration presented an intermediate response, achieving a peak η of 1.27 and a CBR of 13.84%, demonstrating composite behaviour where stress redistribution occurs between the upper and lower layers.
- Fig. 10 further illustrates how η varies with reinforcement depth. The sandy subgrade shows a steep η gradient, with maximum efficiency at 0.3H. This supports earlier observations that vertical stresses are most effectively intercepted near the surface, particularly in cohesionless media where rapid saturation and frictional degradation are critical concerns [83, 159–161].

3.7.3 Implications for Design and Practice

This consolidated analysis presents several actionable insights for geotechnical and pavement engineers seeking to optimize subgrade performance under tropical and moisture-vulnerable conditions:

- GT should be prioritized for reinforcement applications in saturated, fine-grained, and layered subgrades due to its superior full-plane engagement, moisture resistance, and ability to limit lateral deformation. Its consistent performance across all tested configurations highlights its versatility and reliability.
- In sandy subgrades, geotextile placement at 0.3H resulted in the highest performance gain, with a η of 2.02. This indicates a doubling of the soaked CBR, highlighting GT's effectiveness in cohesionless, high-permeability soils where early saturation can rapidly degrade strength. For such soils, shallow placement ensures early stress interception and lateral restraint, which is particularly important for light to medium-traffic unpaved roads.
- For lateritic subgrades, the optimum placement depth shifts to 0.5H, where the geotextile engages with deeper shear zones and mitigates strength loss under saturation. While the absolute CBR is lower compared to sandy soil, the η of 1.52 illustrates efficient reinforcement even under adverse moisture conditions.
- In composite layered systems (e.g., 50:50 sand-over-laterite), a divergence was observed: CBR peaked at 0.5H, while η was highest at 0.3H. This emphasizes the need for context-specific depth optimization, where the designer must weigh whether absolute strength or reinforcement efficiency is more critical based on expected loading and environmental exposure.
- Finally, the use of η as a decision metric offers a cost-performance optimization tool, guiding the selection of material type and placement depth. This is particularly relevant for sustainable pavement design, where economic use of materials aligns with long-term durability objectives, supporting broader infrastructure targets under SDG 9 (Industry, Innovation, and Infrastructure) and SDG 11 (Sustainable Cities and Communities).

4 Conclusions

This research comprehensively investigated the effectiveness of geosynthetic reinforcement in enhancing the strength performance of tropical subgrades, specifically evaluating lateritic, sandy, and layered sand-over-laterite configurations under soaked and unsoaked conditions using the CBR test. The key findings derived from this detailed study offer significant implications for pavement design, subgrade reinforcement optimization, and sustainable infrastructure development. The following key conclusions are drawn, each highlighting critical practical and theoretical implications:

- Superior reinforcement by GT

GT consistently delivered superior performance relative to geogrid in all examined subgrade scenarios. Its continuous planar structure provided greater lateral confinement, mobilization of tensile strength, and enhanced moisture resistance, significantly elevating soaked CBR values. Particularly notable was the soaked reinforcement efficiency ($\eta = 2.02$) in sandy soils, reflecting more than double the bearing capacity compared to unreinforced conditions. This outcome reinforces GT's suitability in cohesionless soils subject to rapid moisture-induced deterioration.

- Soil-specific optimal reinforcement depths

The optimal reinforcement depth varied distinctly based on soil type, moisture sensitivity, and the selected performance metric (absolute CBR vs. reinforcement efficiency η). Sandy soils achieved peak performance at a shallow reinforcement depth ($0.3H$), aligning reinforcement placement with zones of maximum shear and dilation near the surface. Conversely, cohesive lateritic soils demonstrated peak reinforcement effectiveness at deeper levels ($0.5H$), highlighting the necessity to intercept deeper-seated failure planes and mitigate moisture-induced plasticity.

- Layered systems and interface stabilization

Layered sand-over-laterite subgrades exhibited complex mechanical behaviours, which were significantly influenced by the location of the reinforcement relative to the interfacial zone. The maximum absolute CBR occurred at a $0.5H$ placement, directly at the sand-laterite interface, confirming effective stabilization of the stiffness transition. However, η peaked at a shallower depth ($0.3H$), illustrating the critical trade-offs designers must navigate between maximizing bearing capacity and achieving optimal material efficiency.

- Reinforcement efficiency as a key design tool

The difference between optimal absolute CBR and maximum η highlights the importance of considering both metrics in practical pavement design. For heavy-load or high-traffic roads, prioritizing absolute CBR strength at greater depths (such as layered at $0.5H$) might be necessary. Conversely, in resource-limited or low-volume situations, placing reinforcement at shallower depths to maximize η could be more cost-effective. This dual-metric approach is vital for effectively balancing structural integrity and economic resource use in tropical pavement designs.

- Implications for Sustainable Tropical Pavement Design

This research significantly advances infrastructure resilience and sustainability in tropical areas, aligning closely with Sustainable Development Goals (SDG 9 and SDG 11). By identifying geotextile as the most effective reinforcement material and determining optimal depth strategies for various subgrade conditions, these findings provide practical guidance for professionals seeking to develop durable and resilient pavements. The insights improve infrastructure lifespan, significantly reducing maintenance requirements and resource costs in tropical climates with high moisture fluctuations.

- Recommendations for future research

Future research should extend this study's findings to large-scale repetitive plate load testing and finite element numerical modelling under realistic traffic loading. Such research will refine and validate laboratory-derived guidelines, enabling more precise and long-term predictions of pavement performance. Additionally, exploring the degradation of geosynthetic reinforcement under cyclic loads and sustained saturation conditions will further refine our understanding, supporting more robust, durable, and sustainable infrastructure designs.

In conclusion, this study offers critical insights and novel recommendations for geosynthetic reinforcement strategies specifically tailored to tropical road infrastructures, laying a robust foundation for future research, design optimization, and sustainable construction methodologies. It should be noted that the present study is restricted to woven geotextiles and biaxial geogrids tested under controlled laboratory CBR conditions. The findings may not be directly transferable to other geosynthetic types with different polymer compositions, stiffness characteristics, or aperture geometries, nor to more complex field stratigraphies with heterogeneity, anisotropy, or deep groundwater influence. Furthermore, the CBR tests used here represent quasi-static loading and do not fully capture the effects of repeated traffic loading, long-term degradation, or chemical and environmental ageing. Future work should include a broader range of geosynthetics, more

complex layered and variable subgrade profiles, and validation through large-scale plate load tests and instrumented field trials.

In addition to mechanical performance, future studies should incorporate economic and life-cycle cost analyses to compare the cost-effectiveness of alternative reinforcement materials, depths, and configurations. Linking structural performance indices (CBR and reinforcement ratio η) with cost data will enable the formulation of design recommendations that balance strength, durability, and economic sustainability.

Acknowledgements The authors sincerely thank the technical staff of the Geotechnical Engineering Laboratory for their invaluable help during the experimental phase of this study. Their assistance with sample preparation, equipment calibration, and testing procedures was crucial to the success of this research. The authors also appreciate MTS Fibromat Sdn. Bhd. for generously providing the geosynthetic materials used in this investigation. Their contribution helped ensure the consistency and quality of the reinforcement components, which were vital for achieving reliable and reproducible results.

Funding No funding was received for conducting this study.

Data Availability All data, models, or code that support the findings of this study are available from the corresponding author upon reasonable request.

Declarations

Conflict of interest The authors have no conflicts of interest to disclose that are relevant to the content of this article.

References

1. Adedokun, S.I.; Ganiyu, A.A.; Adedokun, M.A.: Effect of marble dust and steel slag on consistency limits and compaction characteristics of lateritic soil. IOP Conf. Ser. Mater. Sci. Eng. (2019). https://doi.org/10.1088/1757-899X/527/1/012026
2. De, C.J.C.; Gitirana, G.F.N.: Unsaturated soils in the context of tropical soils. Soils Rocks (2021). https://doi.org/10.28927/SR.2021.068121
3. Obianyo, I.I.; Taiwo, I.A.; Dayyabu, A.; Mahamat, A.A.; Amuda, A.; Muoka, A.; Mambo, A.D.; Onwualu, A.P.: Modification of lateritic soil using waste plastics for sustainable road construction. Polymers (2024). https://doi.org/10.3390/polym16192689
4. Oyelami, C.A.; Van, R.J.L.: Geotechnical characterisation of lateritic soils from south-western Nigeria as materials for cost-effective and energy-efficient building bricks. Environ. Earth Sci. (2016). https://doi.org/10.1007/s12665-016-6274-1
5. Quispe, R.J.Q.; Romanel, C.: Stability of unsaturated soil slope subject to rain infiltration using coupled and uncoupled finite element approaches. In: Numerical Methods in Geotechnical Engineering Proceedings of the 8th European Conference on Numerical Methods in Geotechnical Engineering NUMGE 2014, Vol. 2, pp. 1025–1030 (2014)
6. Huang, J.; Hartemink, A.E.: Soil and environmental issues in sandy soils. Earth Sci. Rev. (2020). https://doi.org/10.1016/j.earscirev.2020.103295
7. Ramya, R.: Sandy soil: Advantages and disadvantages. In Advantages and Disadvantages of Sandy Soils (2023).
8. Almeida, B.D.; Coelho, L.M.; Guimarães, A.C.R.; Monteiro, S.N.: Effect of sand addition on Laterite soil stabilization. Materials (2024). https://doi.org/10.3390/ma17246033
9. De, S.J.T.F.; Salvagni, H.K.; Falavigna, S.C.; Dalla, R.F.: Mechanical behavior and durability of a typical frictional cohesive soil from Rio Grande do Sul/Brazil improved with Portland cement. Transp. Geotech. (2022). https://doi.org/10.1016/j.trgeo.2022.100751
10. Guimarães, A.C.R.; Povuação, A.M.; Nascimento, G.D.C.; Monteiro, S.N.; Coelho, L.M.: Assessing the potential of lateritic clayey soils for road infrastructure in tropical regions. Materials (2025). https://doi.org/10.3390/ma18081804
11. Liu, W.-Z.; Zeng, Y.-J.; Yao, Y.-S.; Zhang, J.-H.: Experimental study and prediction model of dynamic resilient modulus of compacted subgrade soils subjected to moisture variation. Yantu Gongcheng Xuebao Chin. J. Geotech. Eng. **41**(1), 175–183 (2019). https://doi.org/10.11779/CJGE201901020
12. Otoko, G.R.; Isoteim, F.-M.; Oyebode, O.J.: Some strength and deformation characteristics of laterite. Electron. J. Geotech. Eng. **21**(24), 7907–7914 (2016)
13. Derksen, J.; Fuentes, R.; Ziegler, M.: Geogrid-soil interaction: experimental analysis of factors influencing load transfer. Geosynth. Int. **30**(3), 315–336 (2023). https://doi.org/10.1680/jgein.21.00110
14. Nagendra, P.K.; Manohara, R.R.; Vijaya, B.S.: A simple approach to analysis of stresses in two layered soil medium for engineering applications. Int. J. Earth Sci. Eng. **5**(6 SPECIAL), 1843–1851 (2012)
15. Afzali-Nejad, A.; Lashkari, A.; Martinez, A.: Stress-displacement response of sand-geosynthetic interfaces under different volume change boundary conditions. J. Geotech. Geoenviron. Eng. (2021). https://doi.org/10.1061/(ASCE)GT.1943-5606.0002544
16. Góngora, I.A.M.G.; Palmeira, E.M.: Assessing the influence of soil-reinforcement interaction parameters on the performance of a low fill on compressible subgrade Part II: influence of surface maintenance. Int. J. Geosynth. Ground Eng. (2016). https://doi.org/10.1007/s40891-015-0042-2
17. Lu, W.; Miao, L.; Wang, F.: Mechanism of geogrid reinforcement based on partially developed soil arch effect and design method. Yanshilixue Yu Gongcheng Xuebao Chin. J. Rock Mech. Eng. **31**(3), 632–639 (2012)
18. Ribeiro, J.; Barroso, M.: Geosynthetics in the renewal of east railway line. In: Mechanisms and Machine Science, Vol. 125 MMS (2023). https://doi.org/10.1007/978-3-031-15758-5_86
19. Eltarabily, M.G.; Selim, T.; Elshaarawy, M.K.; Mourad, M.H.: Numerical and experimental modeling of geotextile soil reinforcement for optimizing settlement and stability of loaded slopes of irrigation canals. Environ. Earth Sci. (2024). https://doi.org/10.1007/s12665-024-11560-y
20. Wu, H.; Yao, C.; Li, C.; Miao, M.; Zhong, Y.; Lu, Y.; Liu, T.: Review of application and innovation of geotextiles in geotechnical engineering. Materials (2020). https://doi.org/10.3390/MA13071774
21. Arjomand, M.A.; Abedi, M.; Gharib, M.; Damghani, M.: An experimental study on geogrid with geotextile effects aimed to improve clayey soil. Int. J. Eng. Trans. B **32**(5), 685–692 (2019). https://doi.org/10.5829/ije.2019.32.05b.10
22. Cuelho, E.V.; Perkins, S.W.: Geosynthetic subgrade stabilization—field testing and design method calibration. Transp. Geotech. **10**, 22–34 (2017). https://doi.org/10.1016/j.trgeo.2016.10.002
23. Aria, S.; Shukla, S.K.; Mohyeddin, A.: Optimum burial depth of geosynthetic reinforcement within sand bed based on numerical investigation. Int. J. Geotech. Eng. **14**(1), 71–79 (2020). https://doi.org/10.1080/19386362.2017.1404202

24. Cicek, E.; Guler, E.; Yetimoglu, T.: Effects of the first reinforcement depth on different types of geosynthetics. Sci. Iran. **26**(1A), 167–177 (2019). https://doi.org/10.24200/sci.2017.4231
25. Ensani, A.; Razeghi, H.R.; Mamaghanian, J.: Effect of reinforcement type and soil moisture content on marginal soil-geosynthetic interactions. Soil Mech. Found. Eng. **59**(4), 314–323 (2022). https://doi.org/10.1007/s11204-022-09817-4
26. Hales, T.C.; Miniat, C.F.: Soil moisture causes dynamic adjustments to root reinforcement that reduce slope stability. Earth Surf. Process. Landforms **42**(5), 803–813 (2017). https://doi.org/10.1002/esp.4039
27. Han, D.; Zhou, Z.; Lei, J.; Lin, M.; Zhan, H.: Field experimental study for layered compactness of subgrade based on dimensional analysis. Geomech. Eng. **29**(5), 583–598 (2022). https://doi.org/10.12989/gae.2022.29.5.583
28. Nunes, G.B.; Portelinha, F.H.M.; Futai, M.M.; Yoo, C.: Numerical study of the impact of climate conditions on stability of geocomposite and geogrid reinforced soil walls. Geotext. Geomembr. **50**(4), 807–824 (2022). https://doi.org/10.1016/j.geotexmem.2022.04.004
29. Liu, C.-N.; Huang, W.-W.; Ho, Y.-H.; Lin, B.-H.: Finite element analyses of geosynthetic-reinforced soil ground under surcharge and probabilistic estimation of the bearing capacity. J. Geoeng. **16**(3), 99–109 (2021). https://doi.org/10.6310/jog.202109_16(3).3
30. Moraci, N.; Cazzuffi, D.; Calvarano, L.S.; Cardile, G.; Gioffrè, D.; Recalcati, P.: The influence of soil type on interface behavior under pullout conditions. Geosynthetics **32**(3), 42–50 (2014)
31. Palmeira, E.M.; Filho, J.M.; Fonseca, E.C.A.: An evaluation of reinforcement mechanical damages in geosynthetic reinforced piled embankments. Soils Rocks (2022). https://doi.org/10.28927/SR.2022.000522
32. Sinha, P.; Anusha, Raj, K.; Kumar, S.; Singh, D.: Mechanical behavior of geotextile and geogrids on soil stabilization: a review. In: Lecture Notes in Mechanical Engineering (2023). https://doi.org/10.1007/978-981-19-2188-9_28
33. Tulebekova, A.; Kusbergenova, Z.; Dosmukhambetova, B.; Bakirova, D.; Tleulenova, G.; Zhumadilov, I.: Effects of geogrid and non-woven geotextiles on the shear behavior of soil. Int. J. Geomate **27**(123), 75–82 (2024). https://doi.org/10.21660/2024.123.4633
34. AASHTO, A.A.: Standard Specification for Classification of Soils and Soil–Aggregate Mixtures for Highway Construction Purposes. Washington, DC (2021)
35. Razouki, S.S.; Salem, B.M.: Impact of soaking-drying cycles on gypsum sand roadbed soil. Transp. Geotech. **2**, 78–85 (2015). https://doi.org/10.1016/j.trgeo.2014.11.003
36. Wang, S.-Y.; Zhong, J.-Z.; Ni, Z.-L.; Zheng, X.-C.: Shear behavior of slurry-foam-conditioned poorly graded sand under pressure. Yantu Lixue Rock Soil Mech. **45**(10), 2879–2888 (2024). https://doi.org/10.16285/j.rsm.2023.1697
37. Xiao, J.; Yan, W.; Qiao, S.; Xie, J.; Fang, Z.; Zhang, Z.: Experimental research on the influence of dry density and moisture content on the shear strength of standard sand. J. Railw. Sci. Eng. **20**(10), 3789–3797 (2023). https://doi.org/10.19713/j.cnki.43-1423/u.T20230768
38. Gu, C.; He, X.; Ge, M.; Liu, Y.: Microstructure evolution of a compacted lateritic silt upon drying–wetting and loading. Can. Geotech. J. **60**(10), 1599–1611 (2023). https://doi.org/10.1139/cgj-2022-0352
39. Lim, B.F.; Siemens, G.A.: Shear strength of a swelled soil examining influence of swelling boundary conditions. In: Unsaturated Soil Mechanics from Theory to Practice Proceedings of the 6th Asia Pacific Conference on Unsaturated Soils, pp. 299–303 (2016). https://doi.org/10.1201/b19248-47
40. Bai, W.; Zhang, W.; Kong, L.; Fan, H.; Guo, A.; Xu, G.: Effect of soaking time of dithionite–citrate–bicarbonate solution on strength and deformation characteristics of lateritic soil. J. Rock Mech. Geotech. Eng. **15**(11), 3039–3049 (2023). https://doi.org/10.1016/j.jrmge.2023.02.003
41. Ng, C.W.W.; Akinniyi, D.B.; Zhou, C.; Chiu, C.F.: Comparisons of weathered lateritic, granitic and volcanic soils: compressibility and shear strength. Eng. Geol. **249**, 235–240 (2019). https://doi.org/10.1016/j.enggeo.2018.12.029
42. BS 1377: Part 2 BS: BS 1377-2:1990 Methods of Test for Soils for Civil Engineering Purposes—Part 2: Classification Tests. London (1990)
43. BS 1377: Part 4 BS: BS 1377-4:1990 Methods of Test for Soils for Civil Engineering Purposes—Part 4: Compaction-Related Tests. London (1990)
44. Daou, A.; Chehab, G.; Saad, G.; Hamad, B.: Experimental and numerical investigations of reinforced concrete columns confined internally with biaxial geogrids. Constr. Build. Mater. (2020). https://doi.org/10.1016/j.conbuildmat.2020.120115
45. Liu, G.; Zhao, M.; Liu, K.; Connolly, D.P.; Jiang, X.; Zhang, L.: Comparative study of performance of wicking and conventional railway geotextiles under the synergetic simulation of train loads and flooding. Constr. Build. Mater. (2023). https://doi.org/10.1016/j.conbuildmat.2023.132840
46. Negi, M.S.; Singh, S.K.: Experimental and numerical studies on geotextile reinforced subgrade soil. Int. J. Geotech. Eng. **15**(9), 1106–1117 (2021). https://doi.org/10.1080/19386362.2019.1684654
47. Srivastava, S.; Balunaini, U.: A comparative study on effectiveness of geogrid and geotextile reinforcement in expansive subgrades of flexible pavements. Geotechnical Special Publication, 2025-March (GSP 363), pp. 303–313 (2025). https://doi.org/10.1061/9780784485965.027
48. Wimalasena, K.; Gallage, C.; Jayalath, C.; Churchill, J.: Monotonic loading test to investigate the benefits of composite geogrids for subgrade improvement. In: Lecture Notes in Civil Engineering, Vol. 193 (2022). https://doi.org/10.1007/978-3-030-87379-0_35
49. Abu-Farsakh, M.; Hanandeh, S.; Mohammad, L.; Chen, Q.: Performance of geosynthetic reinforced/stabilized paved roads built over soft soil under cyclic plate loads. Geotext. Geomembr. **44**(6), 845–853 (2016). https://doi.org/10.1016/j.geotexmem.2016.06.009
50. Abu-Farsakh, M.Y.; Akond, I.; Chen, Q.: Evaluating the performance of geosynthetic-reinforced unpaved roads using plate load tests. Int. J. Pavement Eng. **17**(10), 901–912 (2016). https://doi.org/10.1080/10298436.2015.1031131
51. Eissa, A.; Alfaro, M.; Bartz, J.R.; Bassuoni, M.T.; Bhat, S.: Soil-reinforcement interaction of a geogrid–geotextile composite. Int. J. Geosynth. Ground Eng. (2023). https://doi.org/10.1007/s40891-023-00506-2
52. Mithila, S.; Fernando, A.; Jayakody, S.; Gui, Y.; Gallage, C.; Shahkolahi, A.; Chow, R.; Priyankara, N.: Effect of granular layer properties on the stabilisation of weak subgrade with geosynthetics. In: Lecture Notes in Civil Engineering, Vol. 409 LNCE (2025). https://doi.org/10.1007/978-981-97-8241-3_10
53. Walkenbach, T.N.; Han, J.; Parsons, R.L.; Li, Z.: Effect of geogrid stabilization on performance of granular base course over weak subgrade. Geotechnical Special Publication 2020-Febru (GSP 318), pp. 527–535 (2020). https://doi.org/10.1061/9780784482810.055
54. Deshmukh, R.; Patel, S.; Shahu, J.T.: Finite element modeling of geogrid-reinforced unpaved road. In: Lecture Notes in Civil Engineering, Vol. 149 (2021). https://doi.org/10.1007/978-981-16-1303-6_16

55. Fernando, A.; Mithila, S.; Jayakody, S.; Gui, Y.; Gallage, C.; Shahkolahi, A.; Priyankara, N.: Assessment of geogrid reinforcement on the performance of stabilized subgrades under different loading conditions. In: Lecture Notes in Civil Engineering, Vol. 409 LNCE (2025). https://doi.org/10.1007/978-981-97-8241-3_11
56. Sakleshpur, V.A.; Prezzi, M.; Salgado, R.; Siddiki, N.Z.; Choi, Y.S.: Large-scale direct shear testing of geogrid-reinforced aggregate base over weak subgrade. Int. J. Pavement Eng. **20**(6), 649–658 (2019). https://doi.org/10.1080/10298436.2017.1321419
57. BS 1377: Part 9 BS: BS 1377-9:1990 Methods of Test for Soils for Civil Engineering Purposes—Part 9: In-situ Tests. London (1990)
58. Anjos, R.; Carlos, D.M.; Gouveia, S.; Pinho-Lopes, M.; Powrie, W.: Soil–geosynthetic interaction under triaxial conditions: shear strength increase and influence of the specimen dimensions. Int. J. Geosynth. Ground Eng. (2023). https://doi.org/10.1007/s40891-023-00502-6
59. Marto, A.; Oghabi, M.; Eisazadeh, A.: The effect of geogrid reinforcement on bearing capacity properties of soil under static load a: review. Electron. J. Geotech. Eng. J. **18**, 1881–1898 (2013)
60. Singh, M.; Trivedi, A.; Shukla, S.K.: Strength enhancement of the subgrade soil of unpaved road with geosynthetic reinforcement layers. Transp. Geotech. **19**, 54–60 (2019). https://doi.org/10.1016/j.trgeo.2019.01.007
61. Yousuf, S.M.; Khan, M.A.; Ibrahim, S.M.; Ahmad, F.; Samui, P.; Sharma, A.K.: An evaluation of square footing response on lime-treated geotextile-reinforced silty sand: contrasting experimental and computational approaches. Front. Built Environ. (2024). https://doi.org/10.3389/fbuil.2024.1495366
62. Dhanya, K.A.; Musaib, A.; Divya, P.V.: Influence of rainfall on the interface shear strength of unsaturated lateritic soil with geosynthetics. In: Lecture Notes in Civil Engineering, Vol. 152 (2022). https://doi.org/10.1007/978-981-16-1831-4_62
63. Wang, X.Z.; Wang, X.T.; Wang, Z.; Liu, F.; Gao, Q.Q.; Yi, J.T.: Insight and prediction of spudcan elastic stiffness profile in stiff-over-soft clays. Mar. Struct. (2025). https://doi.org/10.1016/j.marstruc.2025.103840
64. Khatti, J.; Grover, K.S.: Relationship between index properties and CBR of soil and prediction of CBR. In: Lecture Notes in Civil Engineering, Vol. 298 (2023). https://doi.org/10.1007/978-981-19-6774-0_16
65. Mohammed, Y.; Paulmakesh, A.; Admasu, B.; Shukri, S.: Relationship between California bearing ratio and other geotechnical properties of sub grade soils. J. Phys. Conf. Ser. (2021). https://doi.org/10.1088/1742-6596/2040/1/012029
66. Pasand, S.A.; Nasrollahi, N.; Asghari-Kaljahi, E.; Majidian, S.: Effect of fine material content on the CBR of Iran saturated soils. Innov. Infrastruct. Solut. (2022). https://doi.org/10.1007/s41062-022-00964-z
67. Manoj, S.; Sampathkumar, V.; Jothi, L.N.; Janani, S.; Nandhini, V.: Interpretation of CBR test consequences for subgrade soil preserved through geo-grid. Int. J. Innov. Technol. Explor. Eng. **9**(1), 3636–3640 (2019). https://doi.org/10.35940/ijitee.A4629.119119
68. Rong, X.; Gao, L.; Han, A.; Ji, C.; Xu, R.; Wu, J.: Fraction of pore pressure and calculation of earth pressure for saturated cohesive soils. Adv. Civ. Eng. (2024). https://doi.org/10.1155/2024/8752954
69. Maha, M.C.; Dutta, T.T.; Bodin, D.; Kodikara, J.: Numerical evaluation of temporal moisture variations in unbound pavements with thin seals. Transp. Geotech. (2022). https://doi.org/10.1016/j.trgeo.2022.100787
70. Maha, M.C.; Dutta, T.T.; Kodikara, J.: Effect of material hydraulic properties on temporal moisture variations and performance of unbound pavements with sprayed seals. Transp. Geotech. (2023). https://doi.org/10.1016/j.trgeo.2023.101071
71. Zegeye-Teshale, E.; Shongtao, D.; Walubita, L.F.: Evaluation of unbound aggregate base layers using moisture monitoring data. Transp. Res. Rec. **2673**(3), 399–409 (2019). https://doi.org/10.1177/0361198119833681
72. Zegeye-Teshale, E.; Holzbauer, M.; Dai, S.: Using ground penetrating radar to monitor seasonal moisture fluctuations in base layers of existing roads. Transp. Res. Rec. **2676**(6), 371–386 (2022). https://doi.org/10.1177/03611981221074360
73. Abhijith, T.K.; Hussain, M.; Sachan, A.: Effect of stress history on stress–strain and volumetric response of laterite soil under undrained and drained conditions. In: Lecture Notes in Civil Engineering, Vol. 55 (2020). https://doi.org/10.1007/978-981-15-0886-8_8
74. Mengue, E.; Mroueh, H.; Lancelot, L.; Eko, R.M.: Mechanical improvement of a fine-grained lateritic soil treated with cement for use in road construction. J. Mater. Civ. Eng. (2017). https://doi.org/10.1061/(ASCE)MT.1943-5533.0002059
75. Okeke, C.; Abbey, S.; Oti, J.; Eyo, E.; Johnson, A.; Ngambi, S.; Abam, T.; Ujile, M.: Appropriate use of lime in the study of the physicochemical behaviour of stabilised lateritic soil under continuous water ingress. Sustainability (Basel). **13**(1), 1–26 (2021). https://doi.org/10.3390/su13010257
76. Ackah, F.S.; Zhuochen, N.; Huaiping, F.: Effect of wetting and drying on the resilient modulus and permanent strain of a sandy clay by RLTT. Int. J. Pavement Res. Technol. **14**(3), 366–377 (2021). https://doi.org/10.1007/s42947-020-0067-3
77. Chakraborty, A.; Goswami, A.: Prediction of California bearing ratio (CBR) from index properties of fine-grained soil. Geotech. Eng. **52**(4), 57–64 (2021)
78. Katte, V.Y.; Mfoyet, S.M.; Manefouet, B.; Wouatong, A.S.L.; Bezeng, L.A.: Correlation of California Bearing Ratio (CBR) value with soil properties of road subgrade soil. Geotech. Geol. Eng. **37**(1), 217–234 (2019). https://doi.org/10.1007/s10706-018-0604-x
79. Nezhad, M.G.; Tabarsa, A.; Latifi, N.: Effect of natural and synthetic fibers reinforcement on California bearing ratio and tensile strength of clay. J. Rock Mech. Geotech. Eng. **13**(3), 626–642 (2021). https://doi.org/10.1016/j.jrmge.2021.01.004
80. Xin, G.; Zhang, A.; Wang, Z.; Shen, Q.; Mu, M.: Influence of humidity state on dynamic resilient modulus of subgrade soils: considering repeated wetting-drying cycles. Adv. Mater. Sci. Eng. (2021). https://doi.org/10.1155/2021/3532935
81. Kou, Y.; Shukla, S.K.; Mohyeddin, A.: Experimental investigation for pressure distribution on flexible conduit covered with sandy soil reinforced with geotextile reinforcement of varying widths. Tunn. Undergr. Space Technol. **80**, 151–163 (2018). https://doi.org/10.1016/j.tust.2018.06.012
82. Majidi, A.; Yazdi, M.: Physical modeling of the effect of using scaled geosynthetic reinforcements on bearing capacity and settlement of strip footing. Int. J. Geomech. (2023). https://doi.org/10.1061/IJGNAI.GMENG-8141
83. Moghaddas, T.S.N.; Sharifi, P.; Dawson, A.R.: Performance of circular footings on sand by use of multiple-geocell or -planar geotextile reinforcing layers. Soils Found. **56**(6), 984–997 (2016). https://doi.org/10.1016/j.sandf.2016.11.004
84. Bhat, M.M.; Pathak, S.; Malik, M.I.; Sharma, S.; Akhter, M.: Quantifying the Influence of Geotextile Placement Depth on Various Layers of Flexible Pavement. Indian Geotechnical Journal (2025). https://doi.org/10.1007/s40098-025-01244-0
85. Negi, M.S.; Singh, S.K.: Improvement of subgrade characteristics with inclusion of geotextiles. In: Lecture Notes in Civil Engineering, Vol. 72 (2020). https://doi.org/10.1007/978-981-15-3677-9_14

86. Abraham, D.; Rakendu, R.; Isaac, D.: Bearing capacity of square footing on hybrid geosynthetic reinforced granular fill over soft soil. In: Lecture Notes in Civil Engineering, Vol. 171 (2022). https://doi.org/10.1007/978-3-030-80312-4_24
87. Anusudha, V.; Rathan, R.T.A.S.; Sunitha, V.; Mathew, S.: Experimental and numerical analysis on shear behavior of coir geotextile reinforced granular subbase-subgrade system. J. Build. Pathol. Rehabil. (2025). https://doi.org/10.1007/s41024-024-00534-z
88. Boban, A.; Gaur, K.; Trivedi, A.: Placement depth and layering effect of geogrid reinforcement in soft subgrade using digital static cone penetration lab test. In: Lecture Notes in Civil Engineering, Vol. 529 LNCE (2024). https://doi.org/10.1007/978-981-97-4852-5_46
89. Zhou, L.; Chen, J.-F.; Wang, R.: Influence of geosynthetics reinforcement on liquefaction and post-liquefaction behaviors of calcareous sand. Ocean Eng. (2024). https://doi.org/10.1016/j.oceaneng.2023.116598
90. Ahmad, H.; Sheble, A.: Effects of including fully wraparound geogrid layers on the load-bearing capacity and settlement of a strip footing resting on sandy soil. Discover Appl. Sci. (2024). https://doi.org/10.1007/s42452-024-05711-w
91. Ji, M.; Wang, J.; Zhao, Y.; Deng, J.; Zheng, Y.: Numerical simulation of the load transfer mechanism of a geosynthetic encased stone column unit cell under embankment loading. Int. J. Geomech. (2024). https://doi.org/10.1061/IJGNAI.GMENG-9393
92. Mir, B.A.; Ashraf, S.: Evaluation of load-settlement behaviour of square model footings resting on geogrid reinforced granular soils. Sustain. Civ. Infrastruct. (2019). https://doi.org/10.1007/978-3-030-01923-5_9
93. Liu, W.; Qu, S.; Nie, Z.; Zhang, J.: Effects of density and moisture variation on dynamic deformation properties of compacted lateritic soil. Adv. Mater. Sci. Eng. (2016). https://doi.org/10.1155/2016/5951832
94. Mu, R.; Huang, Z.; Yao, W.; Cheng, X.; Lei, Y.; Yang, C.: An experimental study of the dynamic characteristics of the undisturbed laterite under graded cyclic loading. Hydrogeol. Eng. Geol. **49**(3), 94–102 (2022). https://doi.org/10.16030/j.cnki.issn.1000-3665.202108053
95. Sarvade, P.G.; Nayak, D.; Sharma, A.; Gogoi, R.; Madhukar, S.: Evaluation of strength characteristics of coconut coir mat reinforced lithomargic clay. Int. J. Civ. Eng. Technol. **9**(8), 1168–1179 (2018)
96. Subramaniam, R.; Banerjee, S.: Three-dimensional numerical analysis of static and cyclic pull-out response of plate anchors in reinforced soft clay. Int. J. Geosynth. Ground Eng. (2024). https://doi.org/10.1007/s40891-024-00548-0
97. Abu-Farsakh, M.; Chen, Q.; Sharma, R.: An experimental evaluation of the behavior of footings on geosynthetic-reinforced sand. Soils Found. **53**(2), 335–348 (2013). https://doi.org/10.1016/j.sandf.2013.01.001
98. Fei, K.; Chen, Y.; Wang, J.-J.: Experimental study on influence of reinforcing modes on behavior of piled embankment. Yantu Gongcheng Xuebao Chin. J. Geotech. Eng. **34**(12), 2312–2317 (2012)
99. Al-Rkaby, A.H.J.; Jaber, A.S.; Odeh, N.A.: Comparative study on the performance of planar and cellular reinforcements for sandy soil. AIP Conf. Proc. (2024). https://doi.org/10.1063/5.0186151
100. Carlos, D.M.; Pinho-Lopes, M.; Lopes, M.L.: Effect of geosynthetic reinforcement inclusion on the strength parameters and bearing ratio of a fine soil. Procedia Eng. **143**, 34–41 (2016). https://doi.org/10.1016/j.proeng.2016.06.005
101. Chen, G.; Qin, Y.; Ma, W.; Liang, K.; Wu, Q.; Juang, C.H.: Liquefaction susceptibility and deformation characteristics of saturated coral sandy soils subjected to cyclic loadings—a critical review. Earthq. Eng. Eng. Vib. **23**(1), 261–296 (2024). https://doi.org/10.1007/s11803-024-2221-4
102. Makkar, F.M.; Chandrakaran, S.; Sankar, N.: Performance of 3-D geogrid-reinforced sand under direct shear mode. Int. J. Geotech. Eng. **13**(3), 227–235 (2019). https://doi.org/10.1080/19386362.2017.1336297
103. Hassan, W.; Alshameri, B.; Nawaz, M.N.; Qamar, S.U.: Experimental study on shear strength behavior and numerical study on geosynthetic-reinforced cohesive soil slope. Innov. Infrastruct. Solut. (2022). https://doi.org/10.1007/s41062-022-00945-2
104. Hassan, W.; Farooq, K.; Mujtaba, H.; Alshameri, B.; Shahzad, A.; Nawaz, M.N.; Azab, M.: Experimental investigation of mechanical behavior of geosynthetics in different soil plasticity indexes. Transp. Geotech. (2023). https://doi.org/10.1016/j.trgeo.2023.100935
105. Christopher, B.R.; Schwarz, L.G.: Performance of geogrids overlying geotextiles in roadway stabilization applications. In: 9th International Conference on Geosynthetics Advanced Solutions for A Challenging World ICG 2010, pp. 1451–1456 (2010)
106. Mankodi, H.: Geocomposite manufactured from PP nonwoven/HDPE geonet. In: Advanced Materials Research, Vol. 622 (2013). https://doi.org/10.4028/www.scientific.net/AMR.622-623.1310
107. Singh, M.; Trivedi, A.; Shukla, S.K.: Effect of geosynthetic reinforcement on strength behaviour of subgrade-aggregate composite system. In: Lecture Notes in Civil Engineering, Vol. 72 (2020). https://doi.org/10.1007/978-981-15-3677-9_7
108. Ziaie, M.R.; Nazari, M.: Effect of utilization of geosynthetic on reducing the required thickness of subbase layer of a two layered soil. World Acad. Sci. Eng. Technol. **73**, 963–967 (2011)
109. Ansari, M.A.; Roy, L.B.: Bearing capacity of a circular footing resting on geogrid reinforced foundation: an experimental and neuro-fuzzy based model. Int. J. Performab. Eng. **18**(10), 690–701 (2022). https://doi.org/10.23940/ijpe.22.10.p2.690-701
110. Ansari, M.A.; Roy, L.B.: Experimental and ANN-based model of footing pressure of a layered soil reinforced with geogrid. Innov. Infrastruct. Solut. (2023). https://doi.org/10.1007/s41062-023-01069-x
111. Tavakoli, M.; Khazaei, M.: Scale effect on the behaviour of geogrid-reinforced soil under repeated loads. Geotext. Geomembr. **45**(6), 603–615 (2017). https://doi.org/10.1016/j.geotexmem.2017.08.002
112. Guo, J.; Han, J.; Zhang, X.; Li, Z.: Experimental evaluation of wicking geotextile-stabilized aggregate bases over subgrade under rainfall simulation and cyclic loading. Geotext. Geomembr. **49**(6), 1550–1564 (2021). https://doi.org/10.1016/j.geotexmem.2021.07.004
113. Lin, C.; Galinmoghadam, J.; Han, J.; Liu, J.; Zhang, X.: Quantifying and incorporating the benefits of wicking geotextile into pavement design. J. Transp. Eng. Part B Pavem. (2021). https://doi.org/10.1061/JPEODX.0000300
114. Yang, B.; Yin, Y.; Yang, C.: Effects of permeable geotextiles of different densities on soil cracking and evaporation behavior. Buildings (2025). https://doi.org/10.3390/buildings15030367
115. Cicek, E.; Buyukakin, V.: Determining geotextile effects on bearing capacity ratio and cost of pavement layers by conducting CBR tests. J. Nat. Fibers **19**(15), 11270–11282 (2022). https://doi.org/10.1080/15440478.2021.2023376
116. Dayana, A.E.; Vasudevan, A.K.: Effect of a coarse material sandwich technique on the behavior of geotextile reinforced clay. In: Lecture Notes in Civil Engineering, Vol. 152 (2022). https://doi.org/10.1007/978-981-16-1831-4_58
117. He, P.; Zhuang, C.; Kong, X.; Liu, B.; Zhang, F.: Mechanical properties and mechanisms of soil-geotextile interface under constant normal stiffness: effect of freezing conditions. Geotext.

Geomembr. **53**(5), 1094–1107 (2025). https://doi.org/10.1016/j.geotexmem.2025.04.003
118. Shafiee, A.; Fathipour, H.; Payan, M.; Jalili, J.; Jamshidi, R.C.: Modulus reduction and damping characteristics of geotextile-reinforced sands. Soil Dyn. Earthquake Eng. (2024). https://doi.org/10.1016/j.soildyn.2024.108641
119. Sreelakshmi, K.R.; Vasudevan, A.K.: Study on performance of geotextile reinforced soils using triaxial compression test. In: Lecture Notes in Civil Engineering, Vol. 137. LNCE (2021). https://doi.org/10.1007/978-981-33-6466-0_17
120. Khan, I.; Sharma, R.K.: Bearing capacity evaluation of square footing resting on reinforced sand. J. Min. Environ. **14**(3), 813–824 (2023). https://doi.org/10.22044/jme.2023.12891.2342
121. Meksi, A.; Sadoun, M.; Youzera, H.; Benmahdi, K.; Bouguenina, O.: Experimental study of the mechanical behavior of dam sediment reinforced by geotextiles and geogrids. Military Tech. Courier Vojnotehnicki Glasnik **72**(2), 855–868 (2024). https://doi.org/10.5937/vojtehg72-48383
122. Shirazi, M.G.; Rashid, A.S.B.A.; Bin, R.N.; Rashid, A.H.B.A.; Moayedi, H.; Horpibulsuk, S.; Samingthong, W.: Sustainable soil bearing capacity improvement using natural limited life geotextile reinforcement—a review. Minerals (2020). https://doi.org/10.3390/min10050479
123. Thamer, L.; Shaia, H.: The effect of geotextile layers and configuration on soil bearing capacity. Math. Model. Eng. Probl. **8**(6), 897–904 (2021). https://doi.org/10.18280/mmep.080608
124. Yalaoui, N.; Trouzine, H.; Meghachou, M.; Miranda, T.: Geotextile reinforced strip footing: numerical modeling and analysis. Math. Model. Eng. Probl. **10**(2), 398–404 (2023). https://doi.org/10.18280/mmep.100202
125. Adajar, M.A.; Gudes, M.; Tan, L.: The use of woven geotextile for settlement reduction of spread footing on granular soil. Int. J. Geomate **16**(58), 211–217 (2019). https://doi.org/10.21660/2019.58.8122
126. Akbar, A.; Bhat, J.A.; Mir, B.A.: Experimental investigation of a reduced-scale square footing model on the geocomposite reinforced layered soil. Indian Geotech. J. **53**(4), 887–903 (2023). https://doi.org/10.1007/s40098-023-00722-7
127. Ding, Y.; Jia, Y.; Wang, X.; Zhang, J.; Luo, H.; Zhang, Y.; Chen, X.: The influence of geotextile on the characteristics of railway subgrade mud pumping under cyclic loading. Transp. Geotech. (2022). https://doi.org/10.1016/j.trgeo.2022.100831
128. Jaswal, P.; Vivek, S.S.K.: Laboratory analysis of the interface shear characteristics of chemically treated coir geotextiles and soil interface. Int. J. Pavement Res. Technol. **18**(3), 614–627 (2025). https://doi.org/10.1007/s42947-023-00369-w
129. Yang, W.; Liu, L.; Bai, Y.; Wang, M.; Chen, J.; Zhu, D.; Wang, S.: Investigation on the moisture migration characteristics of clay under the effect of moisture regulation by geotextile. KSCE J. Civ. Eng. (2025). https://doi.org/10.1016/j.kscej.2024.100032
130. Zaman, M.W.; Han, J.: Sand-Woven geotextile interface shear strengths in different shearing directions. Geotechnical Special Publication 2023-March (GSP 341), pp. 526–535 (2023). https://doi.org/10.1061/9780784484685.053
131. Shukla, S.; Mittal, A.; Tiwari, R.P.; Gupta, K.: Application of nonwoven polyester geotextile for soil improvement in pavements. In: Lecture Notes in Civil Engineering, Vol. 136 LNCE (2021). https://doi.org/10.1007/978-981-33-6444-8_33
132. Abdi-Goudarzi, S.; Ziaie-Moayed, R.; Nazeri, A.: An experimental evaluation of geocomposite-reinforced soil sections. Constr. Build. Mater. (2022). https://doi.org/10.1016/j.conbuildmat.2021.125566
133. Dhanya, K.A.; Divya, P.V.: Hydro-mechanical behaviour of composite-geosynthetic-reinforced soil walls with marginal lateritic backfills through instrumented model tests. Geotext. Geomembr. **53**(1), 474–495 (2025). https://doi.org/10.1016/j.geotexmem.2024.11.007
134. Kiptoo, D.; Aschrafi, J.; Kalumba, D.; Lehn, J.; Moormann, C.; Zannoni, E.: Laboratory investigation of a geosynthetic reinforced pavement under static and dynamic loading. J. Test. Eval. **45**(1), 76–84 (2017). https://doi.org/10.1520/JTE20160170
135. Nazir, R.; Hussain, M.; Sachan, A.: Influence of stress history, strain rate and end effects on undrained shear behaviour and strain localization of laterite soil. Int. J. Geotech. Eng. **14**(8), 888–901 (2020). https://doi.org/10.1080/19386362.2020.1776019
136. Shan, Y.; Ke, X.: Reexamination of collapse failure of fine-grained soils and characteristics of related soil indexes. Environ. Earth Sci. (2021). https://doi.org/10.1007/s12665-021-09678-4
137. Dhanya, K.A.; Vibha, S.; Divya, P.V.: Coupled flow-deformation analysis of MSE wall reinforced with hybrid geogrids. Int. J. Geosynth. Ground Eng. (2023). https://doi.org/10.1007/s40891-023-00466-7
138. Tiwari, N.; Satyam, N.; Puppala, A.J.: Effect of synthetic geotextile on stabilization of expansive subgrades: experimental study. J. Mater. Civ. Eng. (2021). https://doi.org/10.1061/(ASCE)MT.1943-5533.0003901
139. Chen, Q.; Abu-Farsakh, M.; Sharma, R.: Laboratory investigation and analytical solution to the behavior of foundations on geosynthetic reinforced sands. Geotech. Spec. Publ. **230**, 359–370 (2013)
140. Niazi, F.S.; Wangensten-Oye, K.E.: Stacked pile solution for axial load–settlement analysis of driven piles in multi-layered soils. Can. Geotech. J. **57**(6), 851–870 (2020). https://doi.org/10.1139/cgj-2018-0892
141. Jana, A.; Dey, A.: A numerical study of drainage characteristics of nonwoven geotextile on the performance of a reinforced soil wall comprising unsaturated marginal backfill. Geotechnical Special Publication 2024-Febru (GSP 350), pp. 447–458 (2024). https://doi.org/10.1061/9780784485323.045
142. Portelinha, F.H.M.; Zornberg, J.G.: Effect of infiltration on the performance of an unsaturated geotextile-reinforced soil wall. Geotext. Geomembr. **45**(3), 211–226 (2017). https://doi.org/10.1016/j.geotexmem.2017.02.002
143. Cabalar, A.F.; Mustafa, W.S.: Behaviour of sand–clay mixtures for road pavement subgrade. Int. J. Pavement Eng. **18**(8), 714–726 (2017). https://doi.org/10.1080/10298436.2015.1121782
144. Orekanti, E.R.; Buragadda, V.; Salammagari, S.D.; Vallepu, G.S.: Effective utilization of stone powder in road construction using sandwich technique: a laboratory study. Transp. Infrastruct. Geotechnol. **11**(6), 3695–3713 (2024). https://doi.org/10.1007/s40515-024-00448-w
145. Denine, S.; Della, N.; Benziane, M.M.; Feia, S.: Influence of sample preparation method on static liquefaction behaviour of geotextile reinforced sandy soil. SN Appl. Sci. (2022). https://doi.org/10.1007/s42452-022-05139-0
146. Missaoui, S.; Belachia, M.; Meksaouine, M.: Effect of wastes plastic reinforcement on behaviour of sand. Int. Rev. Civil Eng. **9**(5), 188–193 (2018). https://doi.org/10.15866/irece.v9i5.15244
147. Vieira, C.S.; Lopes, M.L.; Caldeira, L.: Soil-geosynthetic interface shear strength by simple and direct shear tests. In: 18th International Conference on Soil Mechanics and Geotechnical Engineering Challenges and Innovations in Geotechnics ICSMGE 2013 1, pp. 3497–3500 (2013)
148. Hatami, K.; Granados, J.; Esmaili, D.; Miller, G.: Reinforcement pullout capacity in mechanically stabilized earth walls with marginal-quality soils. Transp. Res. Rec. **2363**, 66–74 (2013). https://doi.org/10.3141/2363-08
149. Shukla, S.; Tiwari, R.P.; Rajbhar, V.; Mittal, A.: Use of jute geotextile in strength enhancement of soft subgrade soil. In: Lecture Notes in Civil Engineering, Vol. 29 (2019). https://doi.org/10.1007/978-981-13-6713-7_24

150. Nair, A.M.; Latha, G.M.: Effect of sample size and anchorage on the performance of reinforced soil-aggregate systems. Int. J. Geotech. Eng. **10**(1), 1–9 (2016). https://doi.org/10.1179/1939787915Y.0000000010
151. Qu, C.; Cao, Z.; Liu, Z.; Zhou, X.; Li, M.: Frictional characteristics of reinforced soil interfaces based on pullout tests. Shenzhen Daxue Xuebao Ligong Ban J. Shenzhen Univ. Sci. Eng. **41**(4), 499–508 (2024). https://doi.org/10.3724/SP.J.1249.2024.04499
152. Sah, B.K.; Kumar, S.S.; Krishna, A.M.: Investigations on the performance of soft soil subgrade using sand-tyre mattress and geogrid-reinforcement. Int. J. Geosynth. Ground Eng. (2025). https://doi.org/10.1007/s40891-024-00608-5
153. Wang, J.; Qi, H.; Huang, S.; Tang, Y.: Large-scale direct shear test on the interface between geogrid and gravel-soil mixture. Hydrogeol. Eng. Geol. **49**(4), 81–90 (2022). https://doi.org/10.16030/j.cnki.issn.1000-3665.202109022
154. Abdelkader, B.; Ahmed, A.; Mostéfa, B.; Isam, S.: Laboratory study of geotextiles performance on reinforced sandy soil. J. Earth Sci. **27**(6), 1060–1070 (2016). https://doi.org/10.1007/s12583-015-0621-0
155. Kapor, M.; Skejić, A.; Medić, S.; Balić, A.: Experimental evaluation of relative soil–geotextile displacements induced by strip footing pressure on a reinforced foundation bed over soft subgrade. Int. J. Geosynth. Ground Eng. (2023). https://doi.org/10.1007/s40891-023-00503-5
156. Lei, H.; Ma, T.; Feng, S.; Wang, L.: Confinement effect of geocell on the mechanical characteristics of reinforced sand subgrade. Transp. Geotech. (2024). https://doi.org/10.1016/j.trgeo.2024.101336
157. Saha, S.; Pal, S.K.: Experimental and numerical analysis for enhancing bearing capacity of shallow foundation through geotextile implementation. In: Lecture Notes in Civil Engineering, Vol. 449 (2024). https://doi.org/10.1007/978-981-99-8505-0_5
158. Talamkhani, S.; Naeini, S.A.: The undrained shear behavior of reinforced clayey sand. Geotech. Geol. Eng. **39**(1), 265–283 (2021). https://doi.org/10.1007/s10706-020-01490-4
159. Anbarani, M.R.; Abrishami, S.; Bayat, M.: Effect of geogrid reinforcement and soil relative density on performance and contact pressures of ring foundations on sand. KSCE J. Civ. Eng. **27**(12), 5135–5148 (2023). https://doi.org/10.1007/s12205-023-1080-2
160. Kumar, V.K.; Ilamparuthi, K.: Performance of anchor in sand with different forms of geosynthetic reinforcement. Geosynth. Int. **27**(5), 503–522 (2020). https://doi.org/10.1680/jgein.20.00013
161. Saride, S.; Rayabharapu, V.K.; Vedpathak, S.: Evaluation of rutting behaviour of geocell reinforced sand subgrades under repeated loading. Indian Geotech. J. **45**(4), 378–388 (2015). https://doi.org/10.1007/s40098-014-0120-8